uOttawa

L'Université canadienne
Canada's university

FACULTÉ DES ÉTUDES SUPÉRIEURES ET POSTOCTORALES

uOttawa

L'Université canadienne
Canada's university

FACULTY OF GRADUATE AND POSDOCTORAL STUDIES

Viviane Choy

AUTEUR DE LA THÈSE / AUTHOR OF THESIS

M.A.Sc. (Chemical Engineering)

GRADE / DEGREE

Department of Chemical Engineering

FACULTÉ, ÉCOLE, DÉPARTEMENT / FACULTY, SCHOOL, DEPARTMENT

Influence of agitation on the morphology of *Trichoderma reesei* and its correlation with the protein production

TITRE DE LA THÈSE / TITLE OF THESIS

Dr. Jules Thibault

DIRECTEUR (DIRECTRICE) DE LA THÈSE / THESIS SUPERVISOR

CO-DIRECTEUR (CO-DIRECTRICE) DE LA THÈSE / THESIS CO-SUPERVISOR

EXAMINATEURS (EXAMINATRICES) DE LA THÈSE / THESIS EXAMINERS

Dr. Christopher Lan

Dr. Marianne Fenech

Gary W. Slater

Le Doyen de la Faculté des études supérieures et postdoctorales / Dean of the Faculty of Graduate and Postdoctoral Studies

Influence of agitation on the morphology of *Trichoderma reesei* and its correlation with the protein production

Viviane Choy

Thesis submitted to the
Faculty of Graduate and Postdoctoral Studies
In partial fulfillment of the requirements
For the M.A.Sc. degree in Chemical Engineering

Department of Chemical and Biological Engineering
Faculty of Engineering
University of Ottawa

Your file Votre référence
ISBN: 978-0-494-48440-1
Our file Notre référence
ISBN: 978-0-494-48440-1

Abstract

In search for a more sustainable source of fuel, bioethanol has been considered as a primary candidate to achieve this objective. To overcome the competition between food and fuel that is currently developing, bioethanol from lignocellulosic source especially from agricultural residues instead than from corn or sugar cane should be favoured. To hydrolyze the cellulose into fermentable sugars so that they can be used to produce ethanol, cellulase enzyme must be produced efficiently and economically.

The objective of the present research is to contribute toward this goal and, in particular, to study the effect of agitation on cellulase production and on the morphology of *Trichoderma reesei*, the microorganism used to produce this enzyme. A series of eight experiments were conducted in a stirred tank bioreactor (STB) and in a reciprocating plate bioreactor (RPB) at various agitation speeds ranging from 200 to 500 RPM and 0.25 to 1.0 Hz, respectively. For each experiment, image analysis was used to determine changes in morphology of *Trichoderma reesei* throughout the fermentation. The protein productivity was correlated to one morphological parameter, the hyphal growth unit. It was found that in the STB, low agitation (200 and 300 RPM) resulted in lower protein productivity whereas high agitation (500 RPM) was detrimental to the microorganisms. The optimal speed of agitation was determined to be 400 RPM where the highest productivity was achieved. In the RPB, higher agitation speed resulted in a higher productivity and the highest productivity was achieved at 1.0 Hz.

As a second objective, a quick and economical off line method using conventional home blood glucose monitors was developed to measure the glucose concentration during the fungal fermentation of *T. reesei*. Two monitors, OneTouch Ultra and Ascensia Contour, were tested and implemented for the monitoring of the glucose concentration during both flask and bioreactor fermentations of *T. reesei*. OneTouch monitor was found to be more suitable.

Résumé

Dans le but de trouver une source renouvelable de combustible, le bioéthanol apparaît comme un candidat de choix pour atteindre cet objective. Pour éviter la confrontation entre source d'énergie et nourriture qui semble se dessiner présentement, la production de bioéthanol à partir des matières lignocellulosiques, surtout des résidus agricoles plutôt qu'à partir du maïs et de la canne à sucre, doit être encouragée. Pour transformer la cellulose en sucres fermentables capable de produire de l'éthanol, l'enzyme cellulase doit être produite efficacement et économiquement.

Le but du présent projet de recherche est de contribuer à cet objectif et en particulier d'étudier l'effet de l'agitation sur la production de la cellulase et sur la morphologie de *Trichoderma reesei*, le microorganisme utilisé pour produire cette enzyme. Une série de huit fermentations ont été menées dans un bioréacteur avec pales de Rushton (STB) et dans un bioréacteur à plateaux mobiles (RPB) sous diverses vitesses d'agitation allant de 200 à 500 RPM et 0.25 à 1.0 Hz, respectivement. Pour chaque expérience, l'analyse d'image a été utilisée pour déterminer les changements morphologiques du microorganisme *Trichoderma reesei* tout au long de la fermentation. La productivité en protéine a été corrélée à un paramètre morphologique, l'unité de croissance des filaments. Il a été déterminé que dans le STB, une faible agitation (200 et 300 RPM) menait à une plus faible productivité en protéine alors qu'une agitation plus élevée (500 RPM) avait un impact négatif sur les microorganismes. Il a été déterminé que la vitesse optimale d'agitation était 400 RPM pour laquelle la productivité la plus élevée a été obtenue. Dans le RPB, une vitesse d'agitation plus élevée conduit à une plus grande productivité et la plus haute productivité a été obtenue à 1.0 Hz.

Comme deuxième objectif, une méthode hors ligne, à la fois rapide et économique, utilisant des lecteurs de glycémie a été développée pour mesurer la concentration en glucose au cours d'une fermentation de *T. reesei*. Deux lecteurs, le OneTouch Ultra et le Ascensia Contour, ont été testés et utilisés pour suivre la concentration en glucose pour des fermentations en flacons et en bioréacteurs. Le lecteur OneTouch s'est avéré le plus approprié.

Acknowledgements

I would like to express my heartfelt thanks to my supervisor Dr. Jules Thibault for his never-ending guidance, support, encouragement and faith in me. I also want to thank him for giving me this wonderful opportunity to work on this project.

I would like to thank Nilesh Patel for his continuous guidance and support throughout the project. I would also like to thank Philippe Malouf and Raseeka Rahumathulla for their help on the project.

Special thanks go to Dr. David McLean for his advice on the statistical interpretation of the data and to other professors for their encouragement.

I am grateful for the technical support from Louis Tremblay, Franco Ziroldo, and Gerard Nina.

Finally, I would like to thank my family, my aunt Estella and my best friend Bonny for their support and encouragement.

Contributions of Collaborators

Five sets of experiments were performed. The first three sets of experiments consisted in performing 4 fermentations at various agitation speeds in each of the 3 bioreactors: the stirred tank bioreactor (STB), the reciprocating bioreactor (RPB) and the Couette Flow Bioreactor (CFB). The fourth set of experiments consisted of 7 fermentations with various feeding strategies in the STB, and the fifth set of fermentation for testing the home blood glucose monitors.

All sets of experiments, in the STB, RPB and the CFB, were performed in close collaboration with Nilesh Patel and Philippe Malouf. For all these fermentations, my mandate was (1) to prepare the inoculum flasks which were used to inoculate the bioreactors, (2) to assist in setting up the bioreactors, and (3) to help in inoculating the bioreactors. During the fermentation runs, I participated in monitoring the bioreactors, sampling periodically and performing image analysis. At the end of the fermentation, I analyzed the protein activities by filter paper and carboxymethyl cellulase assays.

Two papers for which I am the first authors appear in this thesis. I am also co-author of few other papers that will be the subject of the doctoral thesis of Nilesh Patel submitted roughly at the same time.

Table of Contents

List of Tables

List of Figures

Chapter 1

Introduction

World energy consumption is increasing rapidly and the reserve of fossil fuels is declining as it is a non renewable source. At the same time, emissions of CO_2, SO_2, and NO_x from fossil-fuel combustion are the primary causes of atmospheric pollution (Demirbas, 2008). Hence, there is an increasing trend in the development of sustainable energy with no or little green house net effect and in using renewable sources as much as possible. One of the promising options is biofuels such as bioethanol, biodiesel, and biogas which are produced from biomass, a renewable source. Bioethanol is considered as one of the most important alternatives to gasoline and diesel as it can reduce consumption of fossil fuels by blending the bioethanol into petrol, and reduce emission of greenhouse gases (Demirbas, 2008; Megaritis et al., 2007). The overall process of converting biomass into bioethanol fuel has a neutral or very little net production of greenhouse gases which are mainly blamed for global warming (Figure 1.1).

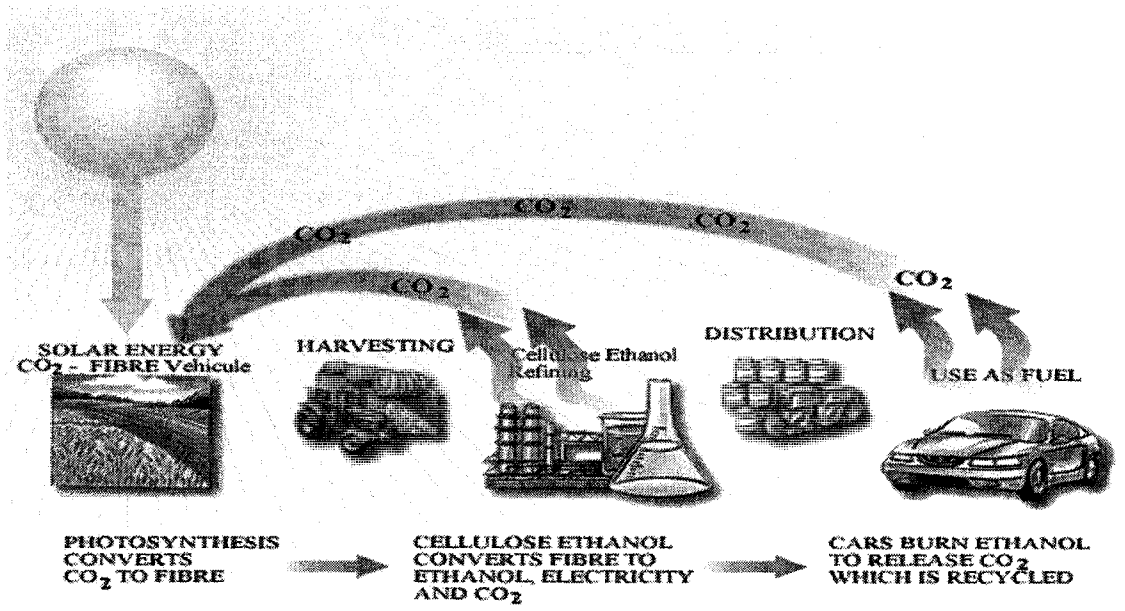

Figure 1.1. The Clean Fuel Cycle: Sustainable Energy with no greenhouse gas effect (www.iogen.ca).

Bioethanol is produced by breaking down parts of biomass contained in corn, sugarcane, and lignocellulosic fibres into simple fermentable sugars and then fermenting these sugars using yeasts or bacteria. Corn grain is currently the most popular feedstock in North America for producing bioethanol. Corn grain contains amylose and amylopectin which are easily broken down into glucose and then fermented into bioethanol (Gray et al., 2006). Sugar cane is another alternative feedstock, very popular in Brazil, mainly composed of sucrose, a dimer made of glucose and fructose, which can be fermented directly without a separate hydrolysis process. However, using corn grain and sugar cane as feedstock will affect the food chain, lowering the amount available for human consumption and also resulting in price increase of certain food products. To partly overcome this potential societal problem, lignocellulosic biomass such as agriculture wastes and wood residues could be used. However, lignocellulosic biomass is mainly composed of 40-50% cellulose, 25–35% hemicellulose, and 15–20% lignin (Gray et al., 2008) which makes it much more difficult to convert it into fermentable sugars. The cost of producing ethanol from lignocellulosic biomass is higher than the production from starch due to the complexity of hydrolyzing the biomass polymer into fermentable sugars (Wyman, 2003), and the production of enzymes necessary in the hydrolysis step.

Conversion of lignocellulosic biomass into bioethanol is a multi-step process as shown in Figure 1.2. Cellulosic feedstock such as corn stover, grass, and straw are first pre-treated mechanically, physically or chemically to break down the fibrous structure. Cellulase enzymes are then added to the pre-treated material to hydrolyze cellulose to glucose, also known as cellulose hydrolysis. The cellulase enzymes are produced in the enzyme production facility through fermenting *T. reesei,* one of the most extensively used industrial microorganisms for the production of cellulase. The sugars are then separated from the unhydrolyzed solids. The latter solids are burned to provide energy for the process, whereas the sugars are fermented to ethanol and the ethanol is recovered by distillation (Philippidis, 1994). In addition to the cellulose, the hemicellulose is now also hydrolyzed to recover additional sugars. The majority of the resulting sugars from this additional hydrolysis step are composed of xylose, a five-carbon sugar. The use of these additional sugars was made possible by the development of genetically-modified yeasts or bacteria that are capable of metabolizing these sugars to produce bioethanol (Dien et al, 2003; Hahn-Hagerdal et al.,

2006). In general, the final sugar mixture from lignocellulosic biomass consists of two thirds glucose and one third xylose (Tolan, 2007). Other five- and six-carbon sugars are also produced but in minor quantity. This work is mainly concerned with the production of cellulase that is essential in the enzymatic hydrolysis of cellulose.

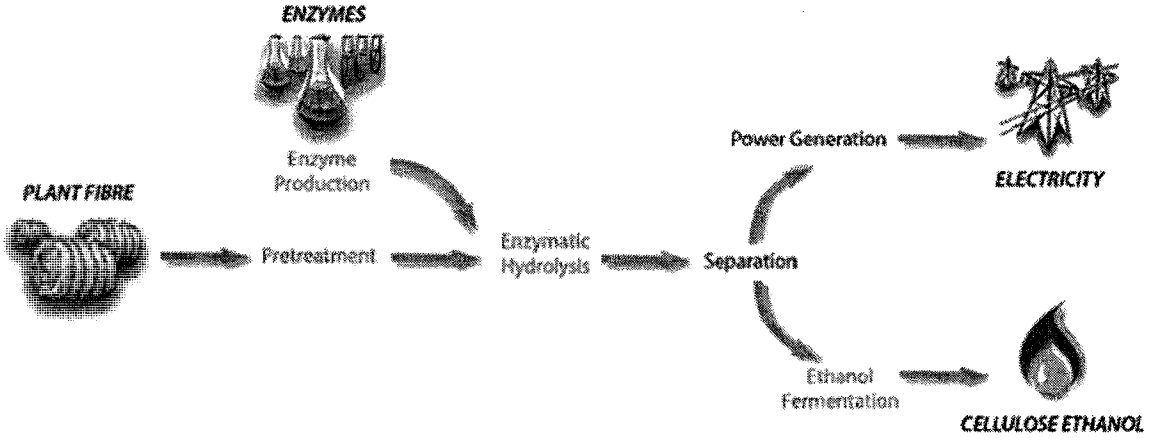

Figure 1.2. Bioethanol production process diagram (www.iogen.ca).

Cellulase can be synthesized by fungi, bacteria (Enari and Markkanen, 1977). Cellulase is not a single enzyme; it is a mixture of the synergistic enzymes, endoglucanases, cellobiohydrolases and β-glucosidase, with variable composition and the degradation of crystalline cellulose to glucose involves the cooperative action of the three enzymes. The endoglucanases and cellobiohydrolases act together to cut the cellulose chains into glucose dimers (cellobiose). The cellobiose is then converted into fermentable glucose molecules by β-glucosidase (Hahn-Hagerdal et al., 2006). The cost of cellulase is about $0.026 to 0.053 per litre ($0.10 to 0.20 per gallon) of bioethanol (Greer, 2005). The cost of the final cellulosic bioethanol can be reduced by improving the yield and quality of cellulase to make it more economically competitive.

Fungal fermentation (Figure 1.3) is a complex system where operating parameters can affect the morphology, growth and product formation which will in turn affect the broth rheology (Schügerl et al., 1998; Cox et al., 1998). The broth rheology has a major impact on the mass and heat transfer, and mixing of the bioreactor which in turn will affect the process conditions. In order to optimize the process, it is important to understand the complex relationship between all these parameters.

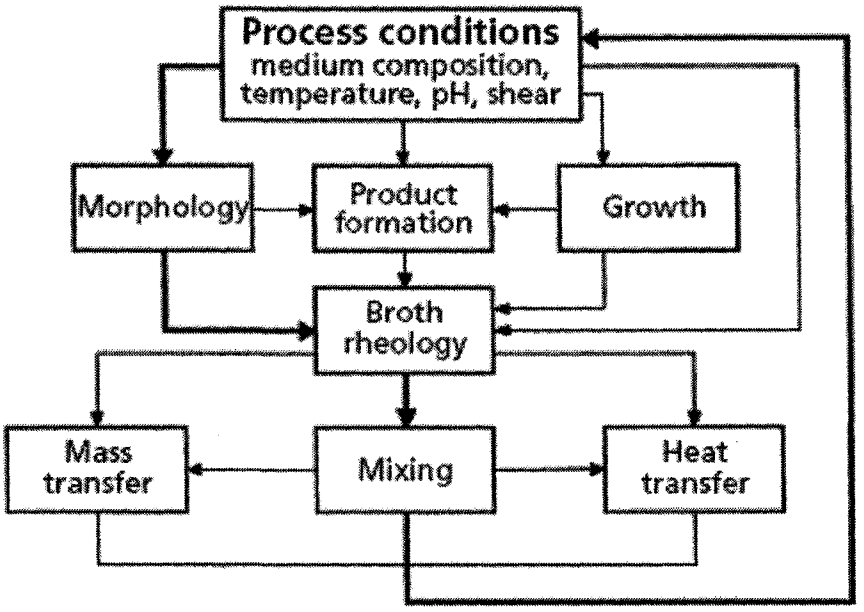

Figure 1.3. Complex interactions between morphology, productivity and process conditions in submerged fermentations of filamentous microorganisms (Cox et al., 1998).

Process conditions (Figure 1.3) such as culture broth composition, glucose concentration, temperature, pH, shear stress, feeding strategies and dissolved oxygen can influence cell growth and product formation. Temperature and pH are measured online while glucose concentration is measured offline. Due to the continuous changing conditions in a bioreactor, it is hard to know the exact value of some of the parameters. Thus the shorter the response time of the equipment or testing time will allow a more accurate knowledge of the conditions (ie: substrate concentration and dissolved oxygen) in the bioreactor during fermentation.

The production of cellulase begins with growing *T. reesei* in a Petri plate. Then, the microorganism is transferred into a flask containing growth medium and a substrate, glucose, and incubated for a few days in a rotary shaker. The flask is then used to inoculate the bioreactor containing growth medium and glucose. The fermentation is initially operated in batch mode where the microorganism is grown. A typical growth curve and the associated glucose consumption and dissolved oxygen profiles observed in a bioreactor are shown in Figure 1.4. The initial lag phase is due to cells adapting to their new environment where it is then followed by an exponential growth phase and an increase in biomass. The nearly

complete consumption of glucose marks the end of the batch phase of the fermentation and the microorganisms then go in a stationary phase and eventually to death phase due to the depletion of glucose. To prevent cell death and, most importantly, to induce the production of cellulase, the mode of operation is switched to fedbatch when the glucose concentration reaches a low value as shown in Figure 1.4. In fedbatch mode, feeding of a lactose solution is initiated. Lactose is used as an enzyme inducer. Hence, a quick and affordable method is required to measure residual sugars in order to start the lactose feeding, i.e. fedbatch phase. Currently, glucose concentration is measured offline by the reducing sugar assay, 3,5-dinitrosalicylic acid (DNS) assay method, and requires time and effort to perform before knowing the actual concentration. Due to the continuous changing conditions in a bioreactor, this time consuming method makes it impossible to determine frequently the exact glucose concentration in the bioreactor. On the other hand, a conventional home blood glucose monitor takes approximately 5 seconds to determine the glucose concentration. These monitors were tested in this investigation to determine if they could provide reliable results for determining glucose concentration in a fermentation broth. This is the subject of Chapter 3 of this thesis.

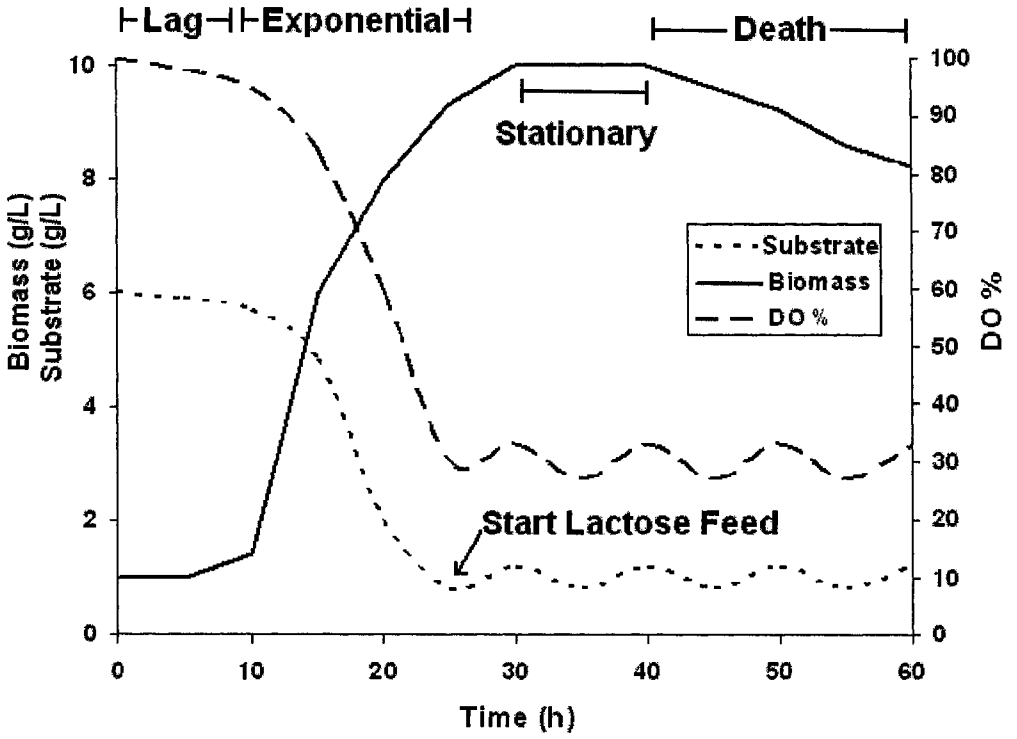

Figure 1.4. Dissolved oxygen, glucose concentration and biomass as a function of fermentation time.

The grand objective of the research project (Figure 1.5) is to study the influence of various operating parameters and how they affect morphology, rheology and protein production (cellulase) during the fermentation in order to improve the yield of cellulase. The scope of the project is very wide and it was performed by a group of researchers. The particular aspect that will mainly be covered in this thesis is the morphology of the microorganism *T. reesei* and its relationship with other process parameters.

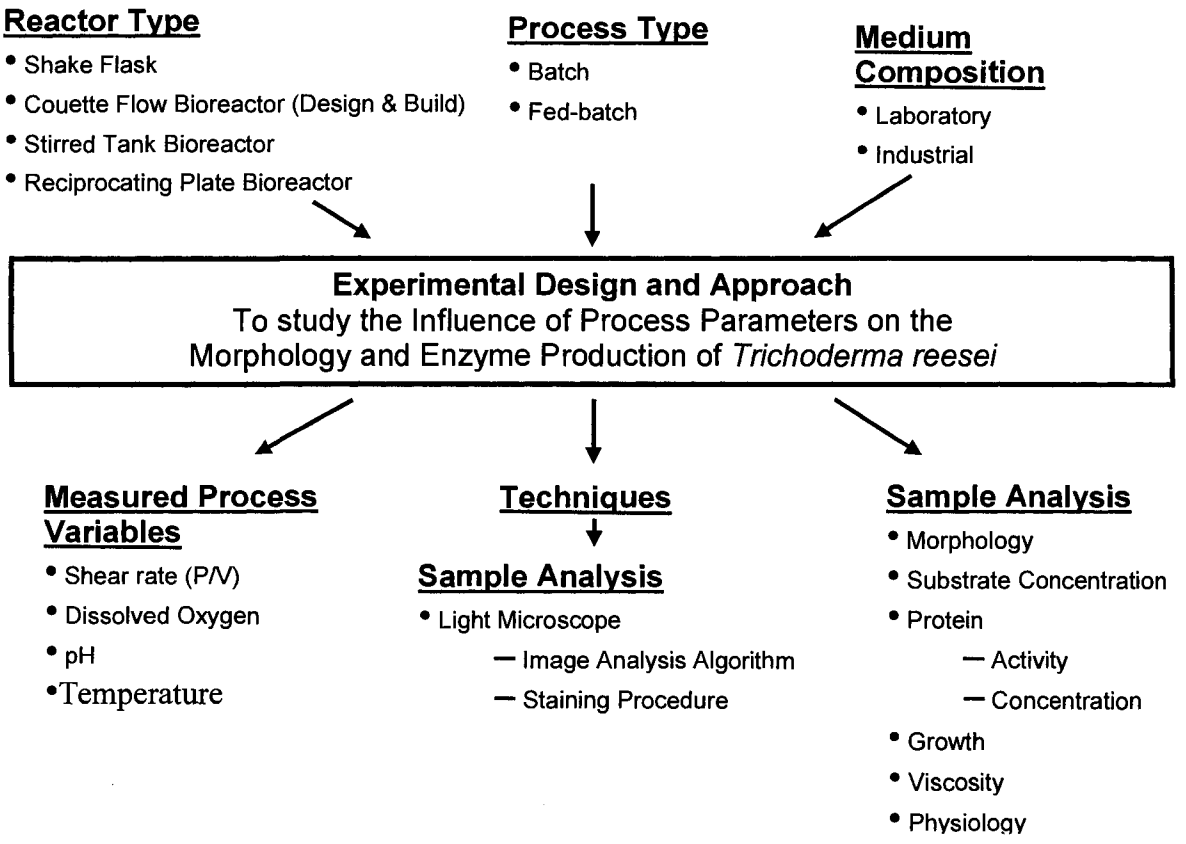

Figure 1.5. Overall research objective.

This thesis is therefore composed of two scientific research papers. The main objective of this research project, presented in Chapter 2, is to study the effect of agitation on the morphology of *T. reesei* and to find a correlation between morphology and the enzyme productivity. Image analysis was used to monitor the changes in morphology during the fermentation. The second objective is to develop a quick and economical method to measure the glucose concentration of a fungal broth and is presented in Chapter 3.

References

Cox, P.W., Paul, G.C., Thomas, C.R. 1998. Image analysis of the morphology of filamentous micro-organisms. Microbiology. 144:817-827.

Demirbas, A. The importance of bioethanol and biodiesel from biomass. 2008. Energy Sources, Part B: Economics, Planning and Policy. 3:177-185.

Dien, B.S, Cotta, M.A., Jeffries, T.W. 2003. Bacteria engineered for fuel ethanol production: current status. Appl. Microbiol. Biotechnol. 63:258-266.

Enari, T.-M. and Markkanen, P. 1977. Production of cellulolytic enzymes by fungi. Adv in Biochemical Engineering/Biotechnology. 5:1-24.

Gray, K.A., Zhao, L., Emptage, M. 2006. Bioethanol. Current Opinion in Chemical Biology. 10:141-146.

Greer, D. 2005. Spinning straw into fuel. Biocycle. 46:61-65.

Hahn-Hägerdal, B., Galbe, M., Gorwa-Grauslund, M.F., Lidén, G., Zacchi, G. 2006. Bio-ethanol - the fuel of tomorrow from the residues of today. Trends in Biotechnology 24: 549-556.

Megaritis, A., Yap, D., Wyszynski, M.L. 2007. Effect of water blending on bioethanol HCCI combustion with forced induction and residual gas trapping. Energy. 32:2396-2400.

Philippidis, G.P. 1994. Chapter 9 Cellulase Production Technology Evaluation of current stays. American Chemical Society.

Shügerl, K., Bayer, T., Niehoff, J., Moller, J., Zhou, W. 1998. Influence of cell environment on the morphology of moulds and the biosynthesis of antibiotics in bioreactors. P. 229-244 In: R.King (ed.), 2nd International Conference on Bioreactor Fluid Dynamics. Elsevier Applied Science. New York.

Tolan, J. 2007. Iogen Corporation, Personal communication.

Wyman, C.E. 2003. Potential synergies and challenges in refining cellulosic biomass to fuels, chemicals, and power, Biotechnol. Prog. 19: 254–262.

Chapter 2

Application of image analysis in the fungal fermentation of *Trichoderma reesei* RUT-C30

Viviane Choy, Nilesh Patel, and Jules Thibault
University of Ottawa
Ottawa (ON) Canada K1N 6N5

Corresponding author: Jules Thibault
Email: Jules.Thibault@uottawa.ca; Tel: 613-562-5800 x6094

Prepared to be submitted to Biotechnology Progress.

Abstract

Trichoderma reesei was grown in a stirred tank bioreactor (STB) and a reciprocating plate bioreactor (RPB) at four different agitation speeds. A semiautomatic image analysis protocol that was developed to characterize the mycelium morphology during the fermentation process based on four morphological types (unbranched, branched, entangled and clumped microorganisms) was applied to study the effect of agitation on the morphology of *T. reesei*. It was shown via statistical validation that broth samples used for image analysis represented the whole population of the fungi in the bioreactor. High shear was found to be damaging to *T. reesei* grown in STB. The much gentler shear produced in RPB was not detrimental to the microorganism even at high agitation speed. Better productivity was obtained for *T. reesei* grown in the STB, and the highest productivity, 0.121 IU/mL h, was obtained at 400 RPM. The morphological parameter, the hyphal growth unit, was correlated to productivity. Understanding the effect of agitation on the morphology and productivity of *T. reesei* could lead to the design of better bioreactors and the selection of operating conditions of bioreactors in order to optimize the production of cellulase.

Introduction

Filamentous microorganisms such as fungi are used extensively in industrial processes for producing antibiotics and many other important proteins and enzymes (Papagianni, 2004). This popularity is due to their high secretion of proteins, which has been correlated with morphological parameters (McIntyre et al., 2001). The fungus *Trichoderma reesei* is one of the most extensively used industrial microorganisms for the production of the enzyme cellulase. High level of secretion when cellulose is used as a substrate endorses widespread applications of the enzyme preparation from *T. reesei* in different fields such as in the hydrolysis of cellulosic biomass in view of its conversion to bioethanol, in the textile industry for improving the quality of cotton and linen garments, in bio-bleaching of cellulose pulp in paper production, among others (Tolan, 1999).

Fungal fermentations are complex systems in which the operating conditions, broth rheology, enzyme production, morphology of the microorganisms and their physiological state are all interrelated (Schügerl et al., 1998; Cox et al., 1998). In order to optimize the process, it is important to understand the complex relationship between these parameters. Image analysis has been used to study the morphological properties of filamentous microorganisms, which have been reported to be related to the protein secretion (Amanullah et al., 2002). However, the relationship between morphology and productivity is not trivial (Grimm et al., 2005). Thus, to properly elucidate the various phenomena involved in fermentations, a multiple-parameter model should ideally be built using morphological and rheological parameters along with the operating conditions to determine the optimal conditions for the production of cellulase.

There are many methods that have been developed to characterize morphologically filamentous fungi and the values of the measured parameters, such as area, perimeters, and diameters were calculated by taking the average of a large sample size. Initially, morphological analyses were performed manually by making measurements on photographs, a procedure that was time consuming and very inaccurate (Thomas, 1992). Digitizing tables were then used and were found to be impractical because they required a large number of measurements to obtain reliable results and were labour-intensive. With the rapid development of computers and digital cameras, image analysis software was developed and found to be more rapid and precise than digitizing tables (Adam and Thomas, 1988). Many semi and completely automatic procedures have been developed for the morphological characterization of filamentous fungi and have been tested for different fungi such as *Aspergillus niger* (Cox and Thomas, 1992), *Penicillium Chrysogenum* (Paul et al., 1992), and *Trichoderma reesei* (Lecault et al., 2007).

It is well known that morphology is affected by the agitation conditions (Amanullah et al., 2002; Jüsten et al., 1996). It has been suggested that protein secretion only occurs at the tip of the hyphae (Amanullah et al., 1999), thus a higher branching frequency or number of tips may lead to an increase in productivity. It has been reported that pelleted growth is preferred over filamentous growth for *Aspergillus terreus* and *Aspergillus niger* for the production of itaconic acid and citric acid, respectively. On the other hand, filamentous growth is preferred for the production of fumaric acid by *Rhizopus arrhizus* (Pazouki and

Panda, 2000). It was also shown that the vacuoles weaken the hyphae and low substrate level made the mycelium more susceptible to fragmentation when exposed to increased agitation (Papagianni et al., 1999). Paul et al. (1994) studied the hyphal vacuolation and fragmentations of *P. chrysogenum* and suggested that hyphal fragmentation is not necessarily due strictly to the shear stress, but also to the physiological state of the microorganisms. A study performed by Jüsten et al. (1996) showed that the vacuolation was independent of the agitation speed, although different impellers produced different amounts of vacuolation.

In this paper, the statistical validation of the sample size required to obtain statistically significant results was studied in order to determine if the obtained values are representative of the true population of the filamentous microorganisms in the bioreactor. Then, the effect of two different types of mixing devices and their intensity of agitation on both the macroscopic and microscopic morphology of *T. reesei* grown in submerged cultures was studied using the image analysis protocol developed by Lecault et al. (2007).

Materials and Methods

Strain

The strain used throughout this work was *T. reesei* RUT-C30 (ATCC 56765) supplied by Iogen Corporation, Ottawa. The glycerol stock solutions of spores were maintained at -80°C and were transferred on potato dextrose agar plates. New plates were prepared every month and kept at 4°C.

Culture

The growth medium contained the following: glucose, 13 g/L; $(NH_4)_2SO_4$, 1.4 g/L; KH_2PO_4, 2.0 g/L; $MgSO_4 \cdot 7H_2O$, 0.6 g/L; $CaCl_2 \cdot 2H_2O$, 0.3 g/L; $FeSO_4 \cdot 7H_2O$, 5.0 mg/L; $MnSO_4 \cdot 7H_2O$, 1.6 mg/L; $ZnSO_4 \cdot 7H_2O$, 1.4 mg/L; $CoCl_2 \cdot 6H_2O$, 2 mg/L and corn steep solids, 6.0 g/L. The pH of the medium was initially adjusted to 5.5 using 10 M NaOH. A solution containing crushed corn steep solids was first autoclaved separately for 60 min to eliminate possible contamination. The complete medium was then autoclaved for 25 minutes. Shake flask cultures were performed with a volume of 500 mL in a 1 L Erlenmeyer flask with three baffles. A spore solution was prepared by scooping the spores from the plate into a microtube containing 1 mL of sterilized water. The spore concentration of the solution

was calculated using a Petroff Hausser counting chamber (Hausser Scientific, Horsham, PA) and an appropriate volume was inoculated in the flask to obtain an initial concentration of approximately 5 x 10^3 spores/mL. The shake flask was incubated in a rotary shaker at 28°C and 200 RPM for 55 h before being transferred into the bioreactor.

Control Strategies

The pH was measured on-line by a pH probe (FermProbe, Broadley-James Corporation, Irvine, CA) whereas the dissolved oxygen (DO) was continuously monitored by a DO sensor (Broadley-James Corporation, Irvine, CA). When the initial glucose was consumed, corresponding to the end of the batch phase, fedbatch was initiated whereby a 150 g/L lactose solution (without nutrients) was added in such a way that the dissolved oxygen was maintained in the vicinity of the 30% set point. An on-off control strategy was used; if the DO was above 30% saturation, a preset flow rate of lactose medium was added to the bioreactor whereas no solution was fed if the DO was below 30%. The comparison was done every 20 s. The preset amount of lactose added was changed manually as the fermentation progressed. A similar on-off control strategy was also used to control the pH at the set point of 4.5 by the addition of 15 vol % NH_4OH.

Bioreactors

Two bioreactor configurations, a stirred-tank bioreactor (STB) and a reciprocating plate bioreactor (RPB), were used to characterize the effect of shear on morphology and physiology of *T. reesei* for the production of cellulase. The STB has a total volume of 22.5 L with a working volume of 17-18 L. The bioreactor has an inner diameter of 228 mm and a column height of 550 mm. Three identical Rushton turbines, mounted on the central shaft, are used for mixing. Four baffles, 375 mm high, 16 mm wide and 1 mm thick, are placed inside the mixing vessel. The RPB, with the identical dimensions as the STB, consists of a stack of perforated plates mounted on a vertically reciprocating shaft used to agitate the vessel contents. The plate stack consists of 6 perforated stainless steel plates, 221 mm diameter and 1.2 mm thick. Each plate is spaced 50 mm apart from one another. The perforations have a diameter of 19 mm and the fractional open area of the plate is 0.35. A more complete description of these two bioreactors can be found in Audet et al. (1996,

1998). Experiments were preformed at 200, 300, 400 and 500 RPM in the STB and at 0.25, 0.50, 0.75, and 1.0 Hz in the RPB.

Image Analysis

An 80 mL sample was withdrawn from the bioreactor periodically during the fermentation to perform various analyses. For image analysis, 1 mL was withdrawn from the 80 mL sample with a cut pipette tip to prevent size exclusion. The 1 mL sample was centrifuged for 15 s at 14000 RPM. The supernatant was removed and the biomass was washed with 1 mL of 0.1 M phosphate-citrate buffer, pH 4.5. A solution of 70 mg fluorescein diacetate (FDA) in 100 mL acetone was prepared and stored in the dark at 4°C. Before each image analysis, 15 µL of the FDA solution was added to 285 µL of the phosphate-citrate buffer. If necessary, the sample was diluted with phosphate-citrate buffer to a final biomass concentration in the range of 0.4 to 4 g/L. One volume of the diluted sample was added to three volumes of the FDA solution. The sample was agitated mildly for 5 min in the dark at 30°C. A 7.5 µL aliquot of the diluted sample was placed on a microscope slide and covered with an 18-mm x 18-mm coverslip for analysis.

A monochrome camera (CoolSnap ES, Roper Scientific, Tucson, AZ) mounted on an Olympus IX81 microscope (Olympus, Melville, NY) was used. The automated stage of the microscope was controlled by Image-Pro® Plus software (Image-Pro® Plus version 5.1, Media Cybernetics, Silver Spring, MD). Sixty sets of frames on each slide were taken pseudo-randomly. The slide was divided into 567 frames and the algorithm controlling the automated stage prevented the same frame to be taken twice. Each frame was grabbed first under bright field. A UV light generated by a mercury lamp was then applied with a filter (490 nm excitation and 520 nm emission) and a second picture was taken. The exposure time of both pictures was 32 ms throughout the analysis.

The analysis subroutines written in VisualBasic embedded within the image analysis software were similar to those reported by Lecault et al. (2007).

Results and discussions

Data validation

Image analysis relies solely on a very small microorganism population of the bioreactor to determine the different morphological parameters that are then attributed to the

whole population of the bioreactor. Nielsen (1996) mentioned that it is difficult to determine the exact population distribution as it will require a large amount of elements to be quantified to validate the calculated morphological distribution in a submerged culture. It is therefore important to ensure that the morphological characteristics of the microorganism obtained via image analysis using a small sample accurately represent the morphological characteristics within the fermenter. In order to postulate that the small volume used for image analysis represents the whole fermentation broth, it is necessary to validate that the subpopulation used for image analysis indeed represents the actual population. Figure 2.1 presents a schematic of the sampling protocol along with the scale of each sample. Firstly, the number of images that need to be analyzed in order to represent very well the microorganism population in the 1 mL sample needs to be determined. Secondly, it is important to validate that the 1 mL withdrawn for image analysis also represents the 80 mL sample that was obtained from the bioreactor. Finally, a third validation is required to show that the microorganism population in the 80 mL sample adequately represents the entire fermentation broth, having a volume in excess of 10 L. Due to the large amount of data obtained, it is important to confirm that the results are statistically significant.

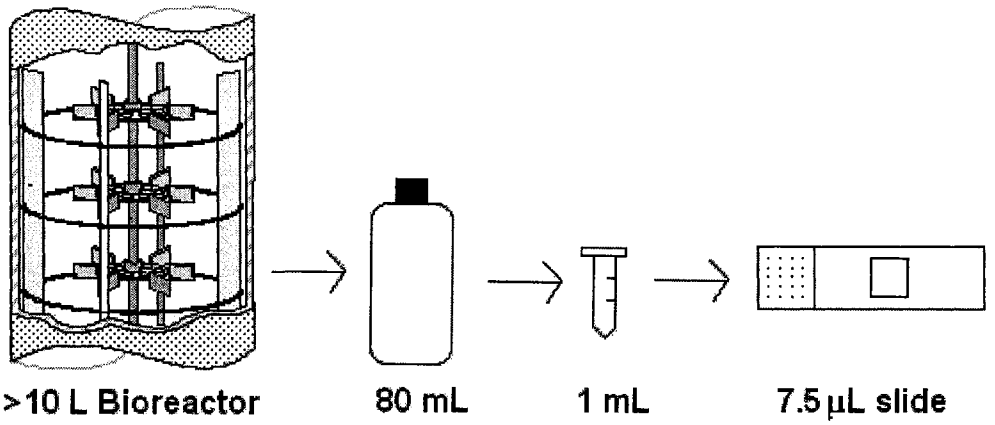

Figure 2.1. Schematic representation of the sampling protocol used for image analysis.

To determine the appropriate number of sets of pictures required for image analysis in order to accurately represent the microorganism population in the 1 mL sample, a test was carried out by acquiring 100 sets of pictures from a sample that was obtained from the bioreactor at 37 h. The time required to acquire these 100 sets of pictures was 60 minutes. Clumps that occupy more than one frame were stitched visually by the operator and a

gradient blend was applied. The set of images were then analyzed using specialized subroutines in ImagePro® software to determine a wide array of morphological and physical parameters.

A population of microorganisms on a slide normally follows a Poisson distribution with respect to their size. However, when large clumps are present, the distribution will vary according to the size of the observation fields and the size of the clumps. In that case, the population follows more closely a binomial distribution but converges to a Poisson distribution when the size of the cumulative observation field increases (Vanhoutte et al., 1995). Since *T. reesei* are present in freely dispersed (unbranched, branched and entangled) and clumped morphology throughout the fermentation, the area fraction of each morphological type was chosen to study the variability of morphological parameters as a function of the number of images analyzed. The results of this analysis are presented in Figure 2.2 in the order that the images were taken. The sample was taken at 36 h from STB at 200 RPM during its batch phase when there is a higher amount of clumps in the bioreactor. It was observed visually that the amount of clumps was higher on one side of the slide; hence the area fractions did not converge to a constant value and showing a slight declining trend as more images were analyzed. Due to the distribution of the microorganisms, it is important to acquire the images across the entire slide. The results show that the area fraction is almost constant when a minimum of approximately 60 images were used for the analysis. To confirm the appropriateness of this number, the average area fractions of the four morphological types for 100 sets of 60 randomly selected images from the 100 images are shown in Figure 2.3 and the mean value and standard deviation are reported in Table 2.1. The random selection avoids the possible bias due to the time of capture and/or the distribution of the microorganisms on the slide. Since there needs to be a compromise between accuracy, storage space, time and the number of images or hyphal elements to be analyzed, 60 images were deemed to be an appropriate number. The number of hyphal elements in the 60 frames ranges from 70 to 300 elements throughout the whole fermentation. During the fedbatch stage of the fermentation, the range of the area of each individual microorganism is narrower than in the batch stage. Also, the clump fraction is minimal, and it was observed visually that the microorganisms are distributed more evenly across the slide. The above statistical test was applied to other measured parameters and was

also repeated with another sample obtained at the end of the batch phase in the bioreactor, and the results showed (refer to Appendix B) similar trends.

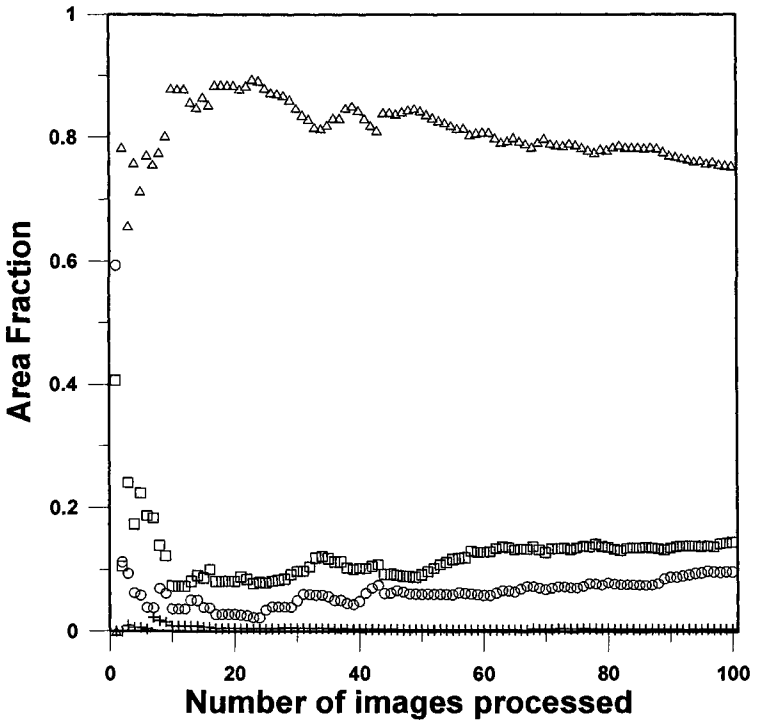

Figure 2.2. Area fractions of unbranched (+), branched (□), entangled (O) and clumped (Δ) morphologies with respect to the number of sequential images analyzed. Experiment performed in STB at 200 RPM and sample taken at 36 h.

Table 2.1. The mean value and the standard deviation of morphological parameters when 60 images were chosen randomly 100 times from the set of 100 images.

Parameters	Mean value
Unbranched	0.004 ± 0.001
Branched	0.157 ± 0.018
Entangled	0.099 ± 0.014
Clumped	0.740 ± 0.029

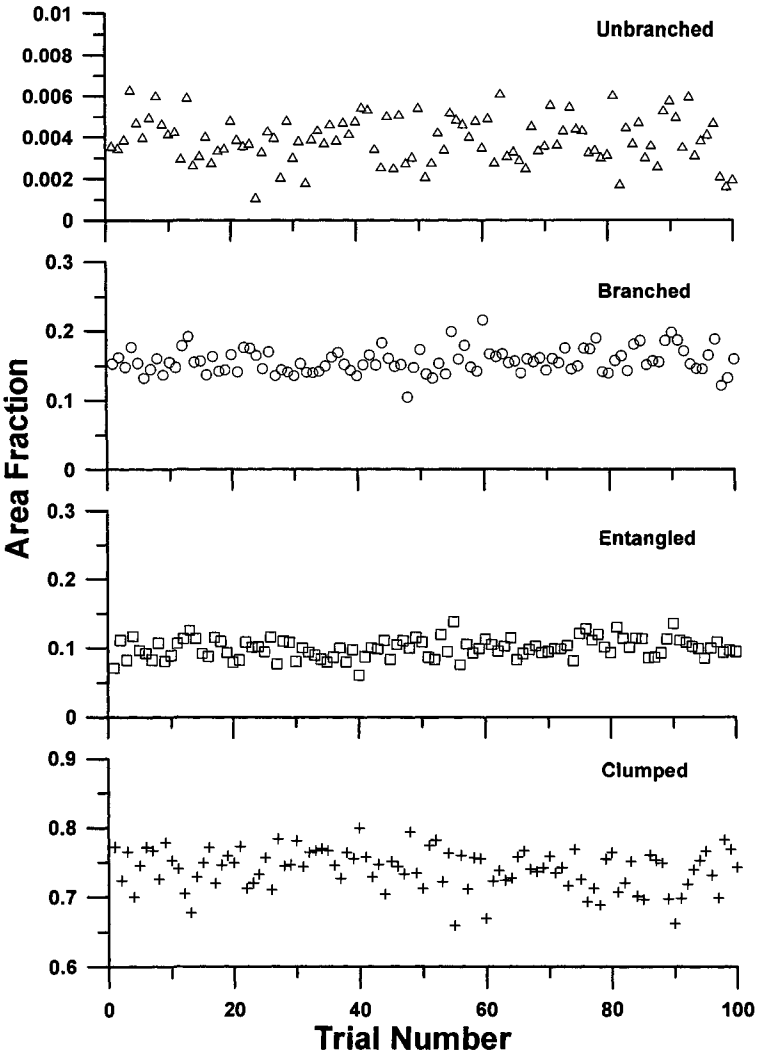

Figure 2.3. Variation of the area fraction of each morphological type, unbranched (+), branched (□), entangled (O) and clumped (Δ), for 100 trials of selecting randomly 60 images amongst the 100 available images. Experiment performed in STB at 200 RPM and sample taken at 36 h.

Component of Variance

Since the variability of the various parameters depends on the slide preparation and the uniformity of the fermentation broth in the bioreactor, a hierarchical design for estimating the different components of the variance is proposed to confirm the postulate that the small volume used for image analysis does indeed represent the fermentation broth and, also, to identify the source of the largest variability in the sampling and image analysis procedure. Pazouki and Panda (2000) found that the reproducibility of morphological data of

batch cultures was poor whereas data for continuous culture showed better reproducibility. Therefore, a 2 x 2 x 3 hierarchical sampling design was performed at two different times during the fermentation: in batch mode at 16 h, and in fedbatch mode at 60 h. This nested hierarchical design is presented schematically in Figure 2.4 and sampling was performed using the following protocol. At the first level, the bioreactor was sampled twice at different locations within the bioreactor with an interval of 30 s. It was assumed that the effect of shear on morphological parameters in the 30 s interval was negligible. At the second level, two 1 mL samples were withdrawn from each of the 80 mL bioreactor sample. At the third level, the image analysis was performed in triplicates whereby three samples were withdrawn from each of the 1 mL sample. Each replicate was assumed to represent the population of the sample.

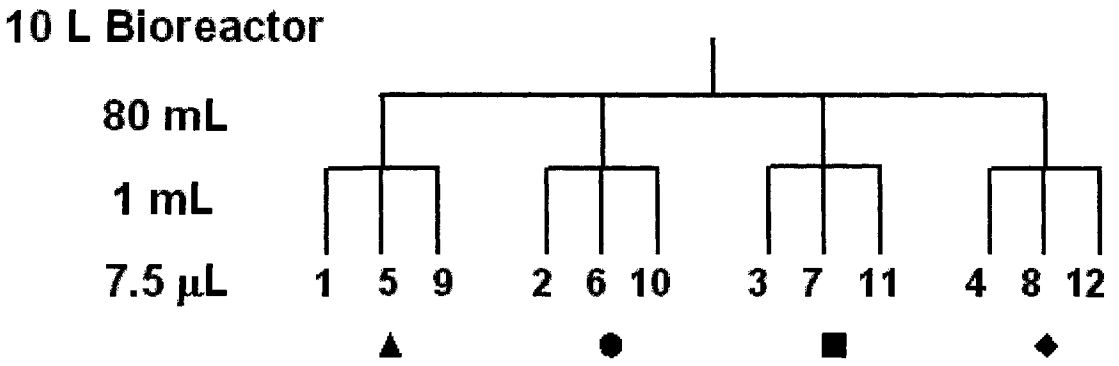

Figure 2.4. Sampling sequence for the 2 x 2 x 3 hierarchical design for estimating the components of the variance. The numbers at the third level indicates the sequence images were acquired and associated symbols in further Figure 2.5.

The image acquisition of the 12 sets of images required a total of 6 h. The number of hyphal objects analyzed for each set of images ranged from 200 to 367 objects. One important morphological parameter, the hyphal growth unit (HGU), was chosen to illustrate the sources of variability from sample to sample. The values of HGU are plotted against the sampling sequence in Figure 2.5, and no noticeable effect of time can be observed. Other parameters such as area fraction for each morphological type, and the diameter were also analyzed and showed no effect of time. Thus, it can be hypothesized that the variation in the parameters can be attributed to the slide preparation at the third level.

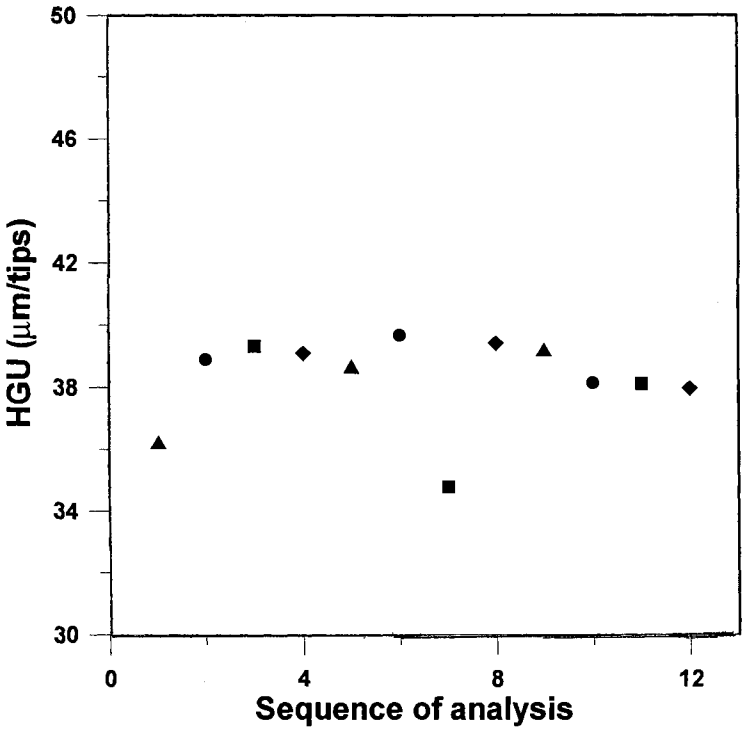

Figure 2.5. HGU for each of the 12 sets of images for the fermentation in the STB at 400 RPM and for samples taken at 60 h.

Table 2.2 presents the analysis of variance (ANOVA) for the HGU analysis. ANOVA is a general technique that can be used to test the hypothesis that the means among different samples are equal, under the assumption that the sampled populations are normally distributed (Montgomery, 2001). From Table 2.2, it can be seen that the variance in the 80 mL sample is negligible meaning the bioreactor is very well mixed. Thus, the sample location has no effect on the whole population. Secondly, the variance of the 1 mL is also negligible, meaning this sample will also represent the population in the bioreactor. The largest variation occurs on the slide. The sample preparation procedures include washing and diluting the sample. The subpopulation distribution across the slides will vary depending on how the droplet and cover glass were placed, in particular when large clumps are present in the sample. Therefore, sample preparation step is very important and the sample should be mixed with a gentle inversion when washing, diluting and staining to minimize any damages on the mycelia resulting in fragmentation. Moreover, to further minimize variance occurring from slide preparation, it is important to acquire images across the entire slide.

The variance of the samples taken at 16 h, partitioned amongst different components, showed similar results to the analysis obtained at 60 h. The analysis was also applied to examine the area fractions and the diameter at the two different time and showed similar results (refer to Appendix C). Thus, the assumption that the subpopulation being used for image analysis represents the population in the bioreactor is deemed valid.

Table 2.2. ANOVA of the HGU for the 12 sets of images for the fermentation in the STB at 400 RPM and for samples taken at 60 h.

Source of Variation	Sum of squares	Degrees of freedom	Mean square	Variance
Average	17931	1		
1st Level	0.510	1	0.510	-0.186*
2nd Level	1.175	2	0.587	-0.151*
3rd level	8.327	8	1.041	1.041
Total	17 941	12		

*The estimate of variance of component is negative but is assumed to be zero or negligible, as suggested by Montgomery (2001), because it is very small.

Viability

The effect of time on the viability was also tested to ensure the vitality of the stain remained effective and the viability did not change throughout the image acquisition step. The test was performed on a large set of 220 images. The time required to acquire these 220 images was 120 min. The average viability of every 5 consecutive frames was calculated in the sequence they were captured. As seen in Figure 2.6, there is a small increase in the average viability for the first sets of 5 frames and then the viability remained relatively stable throughout the remaining of the analysis. The initial increase in viability could be due to insufficient staining time. Therefore, the time spent on capturing the first 60 images will not affect the viability. The average viability of the 220 images is approximately 0.908 ± 0.054.

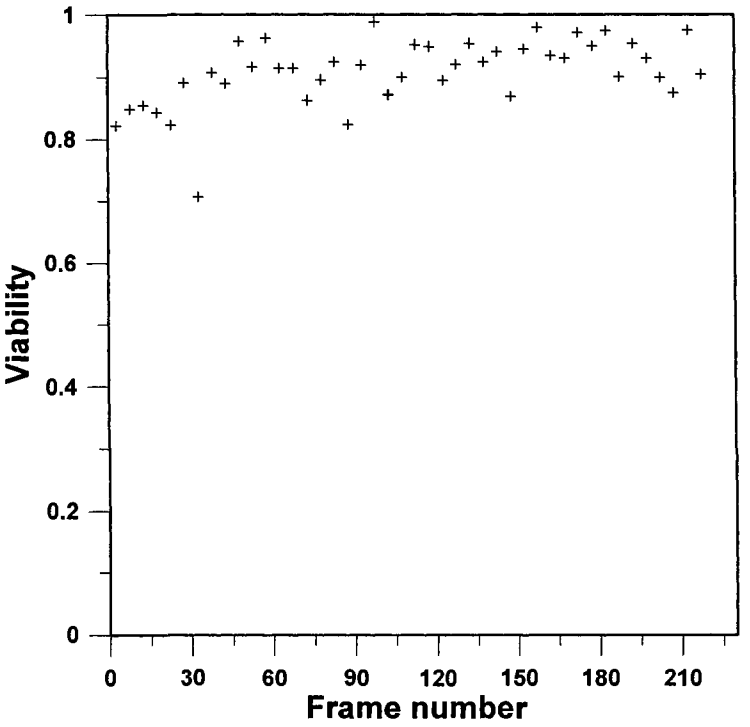

Figure 2.6. Variation of viability with respect to the number of images processed. Each point represents the average of 5 consecutive frames.

In Figure 2.7, the frequency distribution of the mean hyphal diameter of *T. reesei* shows the progress of the population distribution during the fermentation and that the population is nearly normally distributed with a slight skew towards higher hyphal diameters. Similar distributions were observed throughout all fermentations for the hyphal diameter. In addition, all the other morphological parameters also showed either normal or nearly normal distribution. Figure 2.7 also shows that the distribution of the average hyphal diameter slightly shifts to lower values during the fermentation.

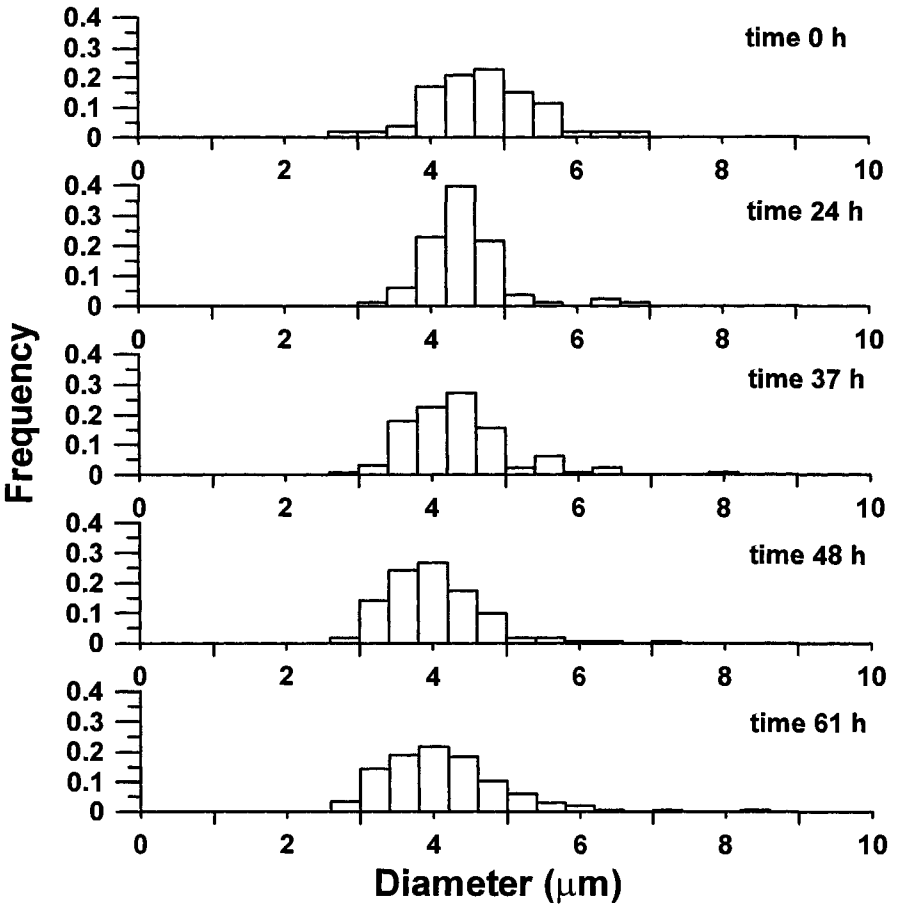

Figure 2.7. Distribution of the hyphal diameter of *T. reesei* in the bioreactor at various times of fermentation in the STB operating at 300 RPM.

Morphological Parameters

The previous analysis has shown that the data determined through the image analysis protocol are representative of the data that prevail inside the bioreactors. In this section, the impact of the type of mixing devices, the intensity of agitation and the fermentation time on some morphological parameters of *T. reesei* is studied. A total of eight fermentations were performed: four in the STB at 200, 300, 400 and 500 RPM, and four in the RPB at 0.25, 0.50, 0.75 and 1.0 Hz.

Area Fraction

The amount of free and clumped mycelia affects the broth rheology and thereby the performance of the bioreactor. Only dispersed mycelia were observed during the

fermentation and classified as unbranched, branched, entangled and clumped. Pelleted mycelia were not present in these fermentations. Mycelia with two tips were classified as unbranched. Those having more than two tips and no holes (created by the overlapping of the hyphae) are classified as branched. Mycelia having more than two tips and less than four holes were classified as entangled, and those with more than four holes were classified as clumped (Paul and Thomas, 1998; Lecault et al., 2007). Figure 2.8 presents the area fraction for the four morphological types as a function of the fermentation time for the lowest and highest speed of agitation in each of the two bioreactors. All eight fermentations, including the four shown in Figure 2.8, began with a high area fraction of clumps. The higher amount of clumps (Figure 2.8-d) in the beginning could be explained by the early growth stages (Pamboukian et al., 2002). Indeed, the inoculum was performed in Erlenmeyer flasks where the shear stress is relatively mild compared to a bioreactor environment. The type of mixing devices and the agitation speed did not appear to have a significant effect on the morphological type in the initial rapid growth stage associated with the batch phase. The same observation was also made by Lejeune et al. (1995). The amount of unbranched and branched microorganisms increases as the fermentation progresses due to the increase fragmentation of clump mycelia. The fragmentations of the clumps occur near the end of the batch phase when the substrate concentration is low, resulting in a decrease in clump fraction area at that point and this decrease continues as the fermentation progresses as the substrate is maintained at a low concentration. High agitation speeds in both STB and RPB resulted in a higher amount of unbranched and branched microorganisms (Figure 2.8 a-b). In the STB, the profiles at 300 and 400 RPM (refer to Appendix E) followed the same trend as the one at 500 RPM. In the RPB, the profile at 0.75 Hz (refer to Appendix E) followed the same trend as for 1.0 Hz, and the profile at 0.50 Hz (refer to Appendix E) was located between 0.25 Hz and 1.0 Hz. The amount of entanglement (Figure 2.8-c) remains almost constant at all agitation speeds in both bioreactors. The amount of clumps decreased more rapidly at higher agitation. However, in the STB at 500 RPM, the clumps did not exceed 0.60, suggesting fragmentation of the microorganisms depends on both the physiological state and the intensity of the shear applied as observed by Paul et al. (1994) with *P. chrysogenum*.

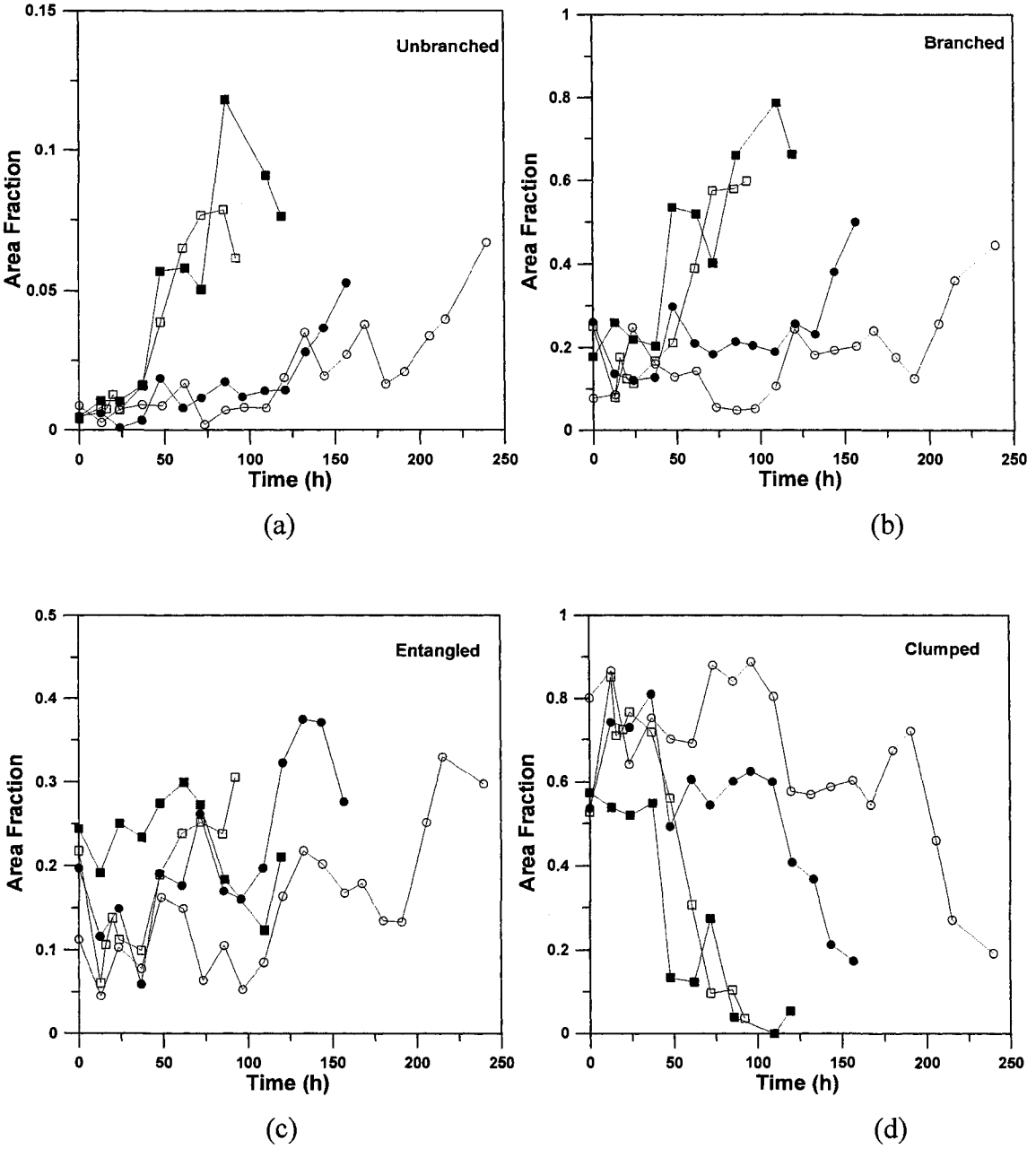

Figure 2.8. Time profiles of area fractions of (a) unbranched (b) branched (c) entangled (d) clumped morphological states in STB at 200 RPM (●), 500 RPM (■), and in RPB at 0.25 Hz (o), and 1.0 Hz (□).

Diameter

Figure 2.9 presents the mean hyphal diameter of free mycelia as a function of time for various speeds of agitation in both STB and RPB. In the STB, the mean hyphal diameter decreases as the fermentation progresses and the mean diameter was higher at the lower agitation. Similar trend was observed at 0.75 and 1.0 Hz in the RPB. Pons et al. (1998) have observed that with *Streptomyces*, aging and septation cause the filament to become thinner by approximately 0.5 μm. However, in the second portion of the fedbatch phase, the mean hyphal diameter progressively increases for the runs at 300, 400 and 500 RPM. This increase is mainly due to the decrease in the power input per unit volume (or shear) as the fermentation progresses. Indeed, for a constant speed of agitation, the progressive volume increase of the fermentation broth during fedbatch leads to a lower power per unit volume. At higher agitation, the growth rate was higher, thus the feeding was higher resulting in a larger increase of liquid volume hence the mean hyphal diameter began to increase near the end of the fermentation. Similar increase in the mean diameter at high agitation rate toward the end of the fermentation has also been observed by Papagianni et al. (1999). In RPB, the sudden large increase in mean diameter from 40 to about 80 h at 0.25 and 0.50 Hz is followed by a sharp decline. The increase could be due to the rate of hyphal extension being lower than the growth rate. It was observed that the thicker mycelia were much more heavily vacuolated, and thus were fragmented earlier causing the sharp decline. Paul et al. (1994) observed similar phenomenon with *P. Chrysogenum*. The increase observed near the end of the fermentation at 0.75 and 1.0 Hz is similar to the trend observed in STB which may be due to the decrease in the power input per unit volume.

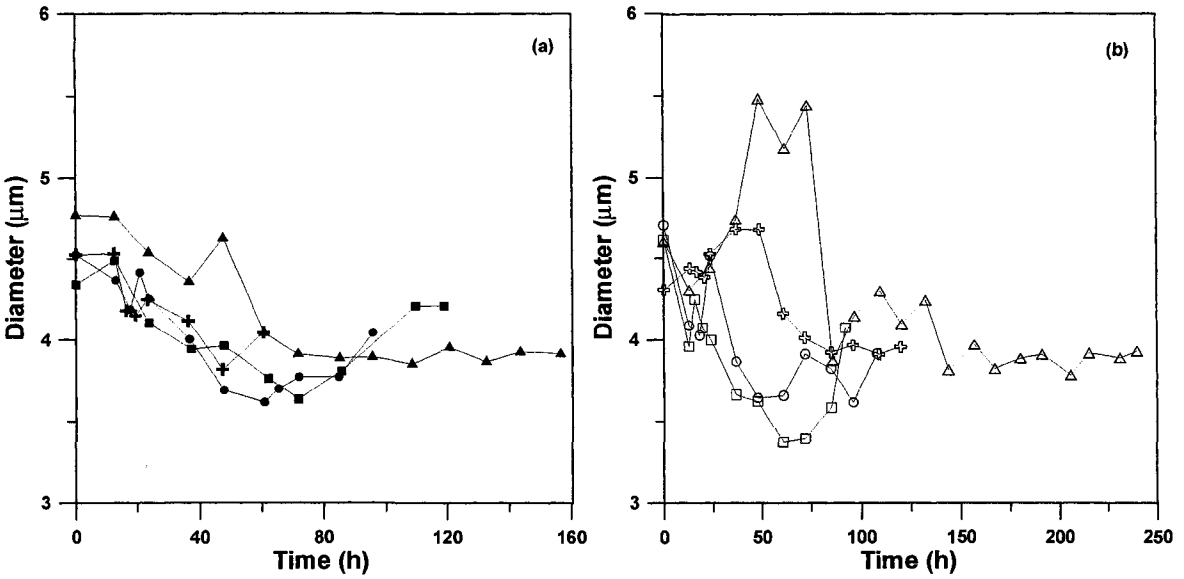

Figure 2.9. Variation of the mean hyphal diameter versus fermentation time in (a) STB at 200 (▲), 300 (+), 400 (●) and 500 (■) RPM; (b) RPB at 0.25 (Δ), 0.50 (+), 0.75 (o) and 1.0 (□) Hz.

General Characteristics

It was observed that the average area increases during the rapid growth phase associated with the batch phase and decreases during the fedbatch period. This is consistent with the observations reported by Li et al. (2002). The average area eventually stabilizes for all four morphological types. Table 2.3 shows some of the general morphological characteristics of *T. reesei* during the fedbatch phase. It should be noted that the different speeds of agitation and types of mixing device did not have a significant effect on the area, perimeter and convex perimeter of *T. reesei* during the fedbatch phase and these morphological parameters stabilized to almost the same values.

Table 2.3. Some general morphological characteristics of *T. reesei* during fedbatch fermentation.

Parameters*	Unbranched	Branched	Entangled	Clumped
Area (μm^2)	84-500	185-2000	460-4620	1270-28000
Perimeter (μm)	60-300	117-930	220-1600	530-3100
Convex perimeter (μm)	60-280	100-590	160-850	320-1500
Perimeter Ratio	0.85-1.00	0.53-0.95	0.46-0.83	0.42-0.71

*Refer to Appendix A where a description of how these morphological parameters are measured is provided.

Hyphal Growth Unit

The hyphal growth unit (HGU), which is defined as the total length of the individual microorganism divided by its number of hyphal tips (Caldwell and Trinci, 1973), is a measure of hyphal branching (Binks et al., 1991). The HGU (Figure 2.10) increased initially and then decreased for all experiments at the end of the batch phase and continued to decrease throughout the fedbatch phase. This phenomenon was also observed by Aynsley et al. (1990) and Neilsen (1993) with *P. Chrysogenum*. Aynsley et al. (1990) suggested that this phenomenon could be due initially to growing cells, extending in length, until the substrates are depleted, at which time the rate of hyphal extension and branching are greatly reduced, and fragmentation begins as a result of the sharp decline in HGU and clumped morphology (Figure 2.8d).

The value at which the HGU stabilizes varied for the type of agitation and speed. For both STB and RPB, the decline in HGU is more rapid at higher agitation and smaller values of HGU are observed. It is also observed that the average dentritic length was shorter at the higher agitation. The continual decrease in the HGU is mostly due to the progressive decrease in length as the fermentation progresses since the number of tips remained close to a constant value during the fedbatch period.

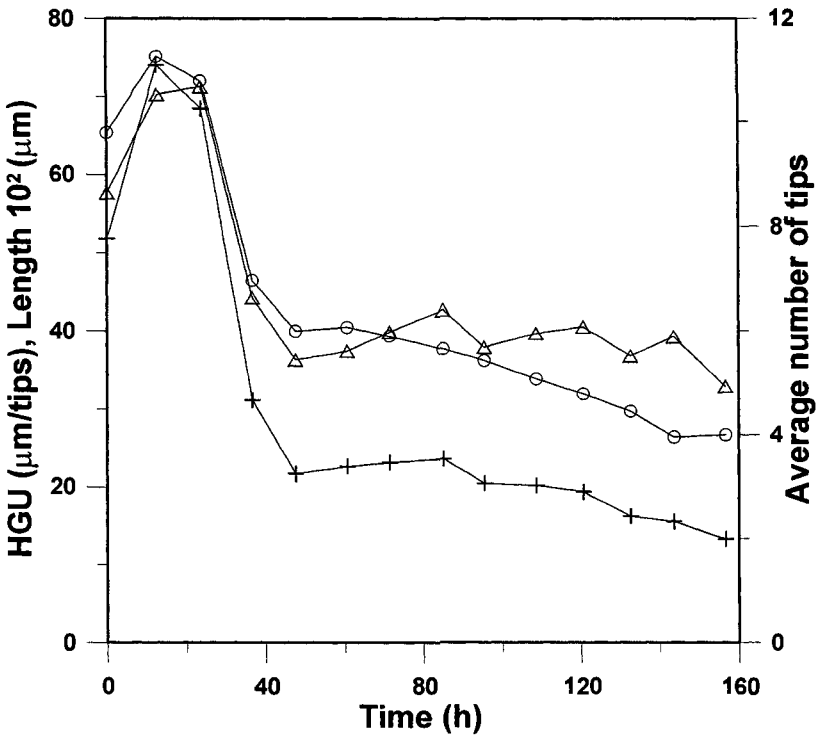

Figure 2.10. Profiles of the average number of tips (Δ), HGU (o) and average dendritic length (+) of the branched mycelia as a function of time for the fermentation conducted in the STB at 200 RPM.

Figure 2.11 shows the typical variation in the protein concentration, the calculated productivity, and the average number of tips as a function of fermentation time. The productivity is calculated via the derivative of the second order fit of the protein concentrated data. The protein production began at the end of the batch phase at the same time when the HGU (Figure 2.10) began to fall drastically. For both bioreactors, the average number of tips per branched mycelia stabilized in the range of 5-6 tips during protein production. There are theories suggesting enzyme is produced at the tips (McIntyre et al., 2001). Wongwicharn et al. (1999) found that extracellular enzyme was related to the number of tips. However, the stable average number of tips did not result in a stable protein production; the productivity went through a maximum and then decreased until the end of the fermentation run.

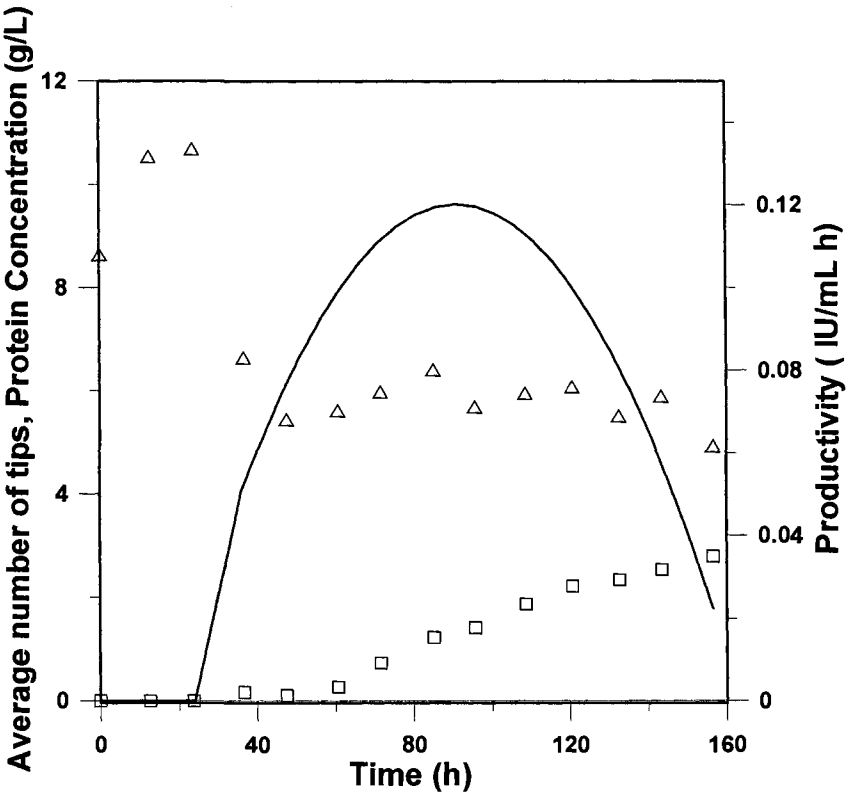

Figure 2.11. Profiles of the protein concentration (□), calculated productivity (—), and average number of tips of the branched mycelia (Δ) as a function of time for the fermentation conducted in the STB at 200 RPM.

Figure 2.12 presents the measured productivity as a function of the HGU values obtained in both bioreactors at different speeds of agitation. For the results of the STB (Figure 2.12a), a general trend is observed where the productivity increases as the HGU decreases. This implies that a large number of tips per unit length should result in more protein production. Highest productivity was achieved at the intermediate speed of 400 RPM. Low agitation, 200 and 300 RPM and very high agitation, 500 RPM resulted in a low productivity. At low agitation, the broth is not as well mixed and there is a lower K_La for oxygen supply hence the microorganisms did not grow as well. The smaller increase in productivity with a decrease in HGU at 500 RPM suggests the high shear is detrimental to the microorganisms due to the fragmentation and associated autolysis, thus generating more dead tips. This observation is consistent with the observations made by König et al. (1981) and Makagianar et al. (1993) with the production of penicillin where the production rate

increased initially with increasing agitation but decreases once the intensity of agitation becomes detrimental to the microorganism, suggesting using intermediate agitation speed. Paul et al. (1994) have also argued that new tips formed by fragmentation are nullified by the autolysis of these newly formed tips.

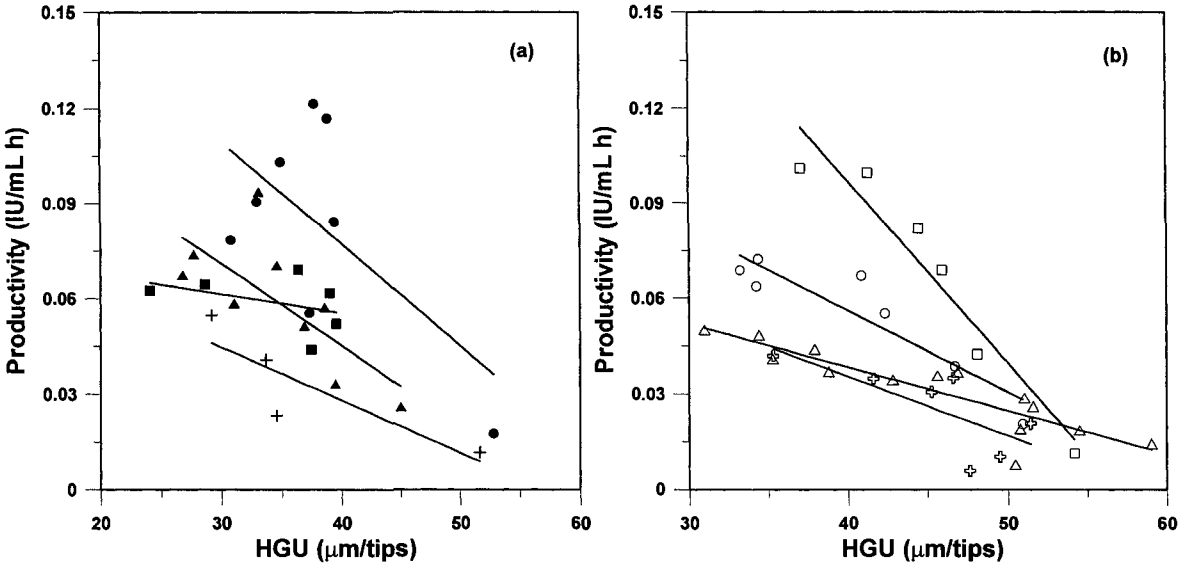

Figure 2.12. The protein productivity as a function of HGU in (a) STB at 200 (▲), 300 (+), 400 (●), and 500 (■) RPM and (b) RPB 0.25 (Δ), 0.50 (+), 0.75 (o), and 1.0 (□) Hz.

For the RPB (Figure 2.12b), a similar trend of a decrease in protein productivity with an increase is HGU is also observed. It appears that in the RPB, the relationship between productivity and HGU is more closely related to the agitation speed than it was in the STB. At higher agitation, there is better mixing of the broth, higher K_La for oxygen supply, hence the microorganisms grow better and hence productivity is higher for higher agitation. Compared to the STB, the shear induced by the reciprocating plates in the RPB is much gentler. Thus, even at 1.0 Hz, it appears that it was not detrimental to the microorganisms.

Conclusion

The validity of the obtained results was confirmed with statistical tests to show that the sample is a true representation of the population of the fungi in the bioreactor. Also, the

viability of the microorganisms remained constant during the analysis, implying that the results are indeed valid for the fungi in the bioreactor. Eight fermentations were performed, four in STB and four in RPB, at various agitation speeds to study the effect of the type of mixing devices and the speed of agitation on *T. reesei*. It was found that during the fedbatch phase, neither the type of mixing devices nor the speed of agitation had an effect on the area and perimeter of each of the four morphological types. They stabilize to almost the same value. Higher agitations in both STB and RPB resulted in a higher growth rate and higher amount of fragmentation which began at the end of the batch phase when substrate concentration was low.

The agitation effect was also correlated with the protein production of *T. reesei*. Protein production began at the end of the batch phase in both bioreactors. It was found that *T. reesei* grown in the STB was able to achieve a higher productivity, with the highest productivity at 400 RPM. In the STB, high shear was shown to be detrimental to the microorganisms; there was a higher amount of fragmentation which resulted in more dead tips that do not produce proteins. In the RPB, higher shear resulted in a higher productivity; this is because the shear produced in the RPB is gentler than in the STB. However, a maximum protein concentration of 3 g/L was obtained at the end of the fermentations, thus the protein productivity is very low, less than 0.13 IU/mL h.

Acknowledgment

The authors are grateful to the Natural Science and Engineering Research Council (NSERC) of Canada for financial support under the Strategic Grant Program. The participation and support of Iogen Corporation is also gratefully acknowledged.

References

Adams, H.L; Thomas; C.R. The use of image analysis for morphological measurements on filamentous microorganisms. *Biotechnol. Bioeng.* 1988, 32, 707-712.

Audet, J.; Lounes, M.; Thibault, J. Pullulan Fermentation in a Reciprocating Plate Bioreactor. *Bioprocess Eng.* 1996, 15, 209-214.

Audet, J.; Gagnon, H.; Lounes, M.; Thibault, J. Polysaccharide Comparison of the Performance of Four Mixing Devices. *Bioprocess Eng.* 1998, 19, 45-52.

Amanullah, A.; Blair, R.; Nienow, AW.; Thomas, CR. Effects of agitation intensity of mycelial morphology and protein production in chemostat cultures on recombinant *Aspergillus oryzae*. *Biotechnol. Bioeng.* 1999, 62, 434-446.

Amanullah, A.; Christensen, L.H.; Hansen, K.; Nienow, A.W.; Thomas, C.R. Dependence of morphology on agitation intensity in fed-batch cultures of *Aspergillus oryzae* and its implications for recombinant protein production. *Biotechnol. Bioeng.* 2002, 7, 815-826.

Aynsley, M.; Ward, A.C.; Wright, A.R. A mathematical model for the growth of mycelial fungi in submerged culture. *Biotechnol. Bioeng.* 1990, 35, 820-830.

Binks, P,R ; Robson, G.D.; Goosey, M.W.; Trinci, A.P.J. Relationships between phosphatidylcholine content, chitin synthesis, growth, and morphology of *Aspergillus nidulans choC*. *Microbiol Lett.* 1991, 83,159-164.

Caldwell, I.Y.; Trinci, A.P.J. The growth unit of the mould *Geotrichum candidum*. *Arch. Microbiol.* 1973, 88, 1-10.

Cox, P.W.; Paul, G.C.; Thomas, C.R Image analysis of the morphology of filamentous micro-organisms. *Microbiology.* 1998,144, 817-827.

Cox, P.W.; Thomas, C.R. Classification and Measurement of fungal pellets by automated image analysis. *Biotechnol. Bioeng.* 1992, 39, 945-952.

Grimm, L.H.; Kelly, S.; Krull, R.; Hempel, D.C. Morphology and productivity of filamentous fungi. *Appl. Microbiol. Biotechnol.* 2005, 69, 375-384.

König, B.; Seewald, C.; Shügerl, K. Process Engineering Investigations of Penicillin Production. *Europ. J. Appl. Microbiol. Biotechnol.* 1981, 12, 205-211.

Jüsten, P.; Paul, G.C.; Nienow, A.W.; Thomas, C.R. Dependence of mycelial morphology on impeller type and agitation intensity. *Biotechnol. Bioeng.* 1996, 52, 672-684.

Lecault, V.; Patel, N.; Thibault, J. Morphological Characterization and Viability Assessment of *Trichoderma reesei* by Image Analysis. *Biotechnol. Prog.* 2007, 23, 734-740.

Lejeune, R.; Neilsen, J.; Baron, G.V. Morphology of *Trichoderma reesei* QM 9141 in submerged cultures. *Biotechnol. Bioeng.* 1995, 47, 60-615.

Li, Z.J.; Bhargava, S.; Marten, M.R. Measurements of fragmentation rate constant imply that the tensile strength of the fungal hyphae can change significantly during growth. *Biotechnol. Lett.* 2002, 24, 1-7.

Makagiansar, H.Y.; Shamlou, P.A.; Thomas, C.R.; Lilly, M.D. The influence of mechanical forces on the morphology and penicillin production of *Penicillium chrysogenum*. *Bioprocess Eng.* 1993, 9, 83-90.

McIntyre, M.; Müller, C.; Dynesen, J.; Nielsen, J. Metabolic engineering of the morphology of *Aspergillus*. *Adv. Biochem. Eng./Biotechnol.* 2001, 73, 103-128.

Montgomery, D.C. Design and Analysis of Experiments 5th ed. Wiley: New York, 2001.

Nielsen J. Modelling the morphology of filamentous microorganisms. TIBTECH 1996, 14, 438–443.

Neilsen, J. A simple morphologically structured model describing the growth of filamentous microorganisms. *Biotechnol. Bioeng.* 1993, 41, 715-727.

Pamboukian, C.R.D.; Guimaraaes, L.M.; Ficciotti, M.C.R. Application of image analysis in the characterisation of *Streptomyces olindensis* in submerged culture. *Braz. J. Microbiol.* 2002, 33, 17-21.

Papagianni, M.; Mattey, M.; Kristiansem. Hyphal vacuolation and fragmentation in batch and fed-btach culture of *Aspergillus niger* and its relation to citric acid production. *Proc. Biochem.* 1999, 35, 359-366.

Papagianni, M. Fungal morphology and metabolite production in submerged mycelial processes. *Biotechnol. Adv.* 2004, 22,189–259.

Paul, G.C.; Kent, C.A.; Thomas, C.R. Viability testing and characterization of germination of fungal spores by automatic image analysis. *Biotechnol. Bioeng.* 1992, 42, 11-23.

Paul, G.C.; Kent, C.A.; Thomas, C.R; Hyphal vacuolation and fragmentation in *Penicillium chrysogenum*. *Biotechnol. Bioeng.*. 1994, 44,655-660.

Paul, G. C.; Thomas, C. R. Characterization of mycelial morphology using image analysis. *AdV. Biochem. Eng. Biotechnol.* 1998, 60, 1-59.

Pazouki, M.; Panda, T. Understanding the morphology of fungi. *Bioprocess Eng.* 2000, 22, 127-143.

Pons, M.N.; Drouin, J.F.; Louvel, L.; Vanhoutte, B.; Vivier, H.; Germain, P. Physiological investigations by image analysis. *J. Biotechnol.* 1998, 65, 3-14.

Thomas, CR. Image analysis: putting filamentous microorganisms in the picture. *Trends in biotechnol.* 1992, 10, 343-348.

Tolan, J. S.; Foody, B. Cellulase from Submerged Fermentation. *Adv. Biochem. Eng./Biotechnol.* 1999, 65, 41-67.

Shügerl, K.; Bayer, T.; Niehoff, J.; Moller, J.; Zhou, W. Influence of cell environment on the morphology of moulds and the biosynthesis of antibiotics in bioreactors. In: R.King (ed.), 2nd International Conference on Bioreactor Fluid Dynamics. Elsevier Applied Science. New York, 1998; pp 229-244.

Vanhoutte, B.; Pons, M.N.; Thomas, C.R.; Louvel, L.; Vivier, H. Characterization of *Penicillium chrysogenum* physiology in submerged cultures by color and monochrome image analysis. *Biotechnol. Bioeng.* 1995, 48, 1-11.

Wongwicharn A.; McNeil B.; Harvey L.M. Effect of oxygen enrichment on morphology, growth, and heterologous protein production in chemostat cultures of Aspergillus niger B1-D. *Biotechnol. Bioeng.* 1999, 65, 416-424

Chapter 3

Blood glucose monitor: an alternative off-line method to measure glucose concentration during fermentations with *Trichoderma reesei*.

Viviane Choy, Nilesh Patel and Jules Thibault*

Department of Chemical Engineering

University of Ottawa, Ottawa (ON), K1N 6N5, Canada

* Author for correspondence. Fax: 613-562-5172; email: Jules.Thibault@uottawa.ca

Key words: Blood Glucose Monitor, Fermentation, Glucose Concentration.

Published July 2007 in Biotechnology Letters 29:1075-1080.

Abstract

Two home blood glucose monitoring meters, OneTouch Ultra and Ascensia Contour, were used to determine the glucose concentration during the fermentations of *Trichoderma reesei* in both flasks and bioreactors. The results, when compared to those given by the 3,5-dinitrosalicylic acid reducing sugar assay, HPLC and YSI 2700 SELECT Biochemistry analyzer, showed that the glucose meters are a quick, reliable and economical alternative method for frequent glucose concentration measurement during fermentation. For *Trichoderma reesei* fermentations, the OneTouch meter was found to be more suitable

Introduction

The quick and rapid determination of glucose concentration is often required in operating many bioprocesses. For example, during the production of cellulase in a fed-batch fermentation of *Trichoderma reesei*, feeding of the enzyme promoter substrate should begin when the glucose concentration reaches a desired value. Another example is carbon catabolite repression by glucose where its rapid feeding can cause a decrease in productivity (Minihane and Brown 1986). On-line glucose systems are not always preferred due to their time delay and instability (Lee et al. 1999). Quick off-line methods are often favoured and can also be used to confirm the on-line measurements.

Some of the widely used techniques to measure glucose are 3,5-dinitrosalicylic acid (DNS) reducing sugar assay, HPLC, and enzyme-based biochemistry analyzers such as YSI 2700 SELECT. These methods provide accurate estimate of glucose concentration. However, they are time consuming and costly which limit their application when rapid and frequent estimates of glucose concentrations are required. Table 2.1 presents a summary of the approximate cost and time required for each method.

An alternative to the above methods is to use a home blood glucose monitor. Home blood glucose monitors are inexpensive, portable and can give results in 5 to 20 s. The procedure is very simple; a droplet of the sample is placed on a test strip that was previously inserted into the meter. The enzymatic reaction between the oxidizing enzyme and the

substrate results in the generation of a current proportional to the glucose concentration in the sample. Glucose oxidase (GOx) is one of the commonly used enzyme with the advantage of having a high glucose specificity, however, it is pH and oxygen dependent (Newman and Turner 2005, Tang et al. 2001, Weibel and Bright 1971). This could be problematic as the pH level and dissolved oxygen tend to vary throughout the fermentation when they are not controlled. Pyrroloquinoline quinine glucose dehydrogenase (PQQ-GDH) is another enzyme used in these biosensors and it has been found to be independent of pH (D'Costa et al. 1986).

Table 3.1. Approximate cost and required time for various glucose analysis.

Method	Materials Required	Capital cost ($ CAD)	Operating cost ($ CAD/100 samples)	Time
DNS[a]	Spectrophotometer	$4 000-$15 000	$60/l DNS reagent	40 min
HPLC	Column Equipment	$500-$1 000 $25 000		25 min
YSI 2700[b]	Equipment	$20 000	$150	2 min
Glucose Monitors[c]	100 Strips		$80-$100	5-20 s

[a]DNS: 3,5-dinitrosalicylic acid reducing sugar

[b]YSI: Yellow Springs Instruments

[c]The monitors are usually provided free of charge when buying measurement strips.

Several researchers have tried using blood glucose monitors for other applications even though they are designed specifically for the analysis of human blood. Nayak and Herman (1997) used glucose meters to monitor the glucose concentration in tissue culture media. Cook et al. (1998) used them to measure the residual sugar in wine and Iversen et al. (2003, 2005) measured the glucose concentration in salmon. Also, FitzGerald and Vermerris (2005) measured the glucose yield from an enzymatic saccharification of maize stover. GlucCell glucose monitoring system (Dunn Labortechnik, GmbH) is based on same principle as glucose blood analyzer. However, the targeted applications are for mammalian and insect cell cultures.

The objective of the current study is to determine the applicability of blood glucose monitors as a rapid alternative method in determining the glucose concentration during

fungal fermentation where other substrates, nutrients and products are present in quantities that vary with time.

Materials and Methods

Glucose solutions

Glucose monitors were first tested with known concentrations of glucose. Aqueous glucose solutions with a pH 4.6 and 8.6 were prepared by adjusting pH with sulphuric acid. Also, solutions of glucose dissolved in the growth medium containing $(NH_4)_2SO_4$, 1.4 g/L; KH_2PO_4, 2.0 g/L; $MgSO_4 \cdot 7H_2O$, 0.6 g/L; $CaCl_2 \cdot 2H_2O$, 0.3 g/L; $FeSO_4 \cdot 7H_2O$, 5.0 mg/L; $MnSO_4 \cdot 7H_2O$, 1.6 mg/L; $ZnSO_4 \cdot 7H_2O$, 1.4 mg/L; $CoCl_2 \cdot 6H_2O$, 2 mg/L and corn steep solids, 6.0 g/L with a pH of 4.8 were prepared. Chemicals were ACS reagent grade and purchased from Sigma-Aldrich.

Flasks fermentations

Trichoderma reesei RUT C-30 (ATCC 56765) was obtained from Iogen Corporation, Ottawa. The culture was grown in 2 L Erlenmeyer flasks containing 1 L of the growth medium with 13 g glucose/L. The pH of the medium was initially adjusted to 5.5 using 10 M NaOH. The flasks were incubated at 28°C and 200 RPM. Filtered samples were diluted to ensure the glucose concentration was within the working range of the meter. To avoid the dependence of pH, 1M citrate buffer (210 g citric acid monohydrate per liter adjusted with NaOH to pH 4.8) was used to adjust the pH to 4.8 by adding 40 µL to 1 mL filtered samples.

Bioreactor

A batch experiment was performed in a homemade stirred tank bioreactor (STB) at 200 RPM with a working volume of 9 L. Air was sparged into the bioreactor at 10 L/min. The bioreactor had an inner diameter of 228 mm and a column height of 550 mm. Three identical Rushton turbines, mounted on the central shaft, were used for mixing. Four baffles, 375 mm high, 16 mm wide and 1 mm thick, were placed inside the mixing vessel. A 450 ml and 55 h old culture of *Trichoderma reesei* RUT C-30 was used to inoculate the bioreactor. The culture medium was the same as for the flask fermentations. A one-sided pH control was performed by the addition of NH_3OH (15% v/v) to prevent the pH to decrease below

4.5. Filtered samples were adjusted with 1M citrate buffer. The biomass weight was determined by dry cell weight method.

Glucose analysis

The glucose concentration was measured by 3,5-dinitrosalicylic acid reducing sugar (DNS) assay (Ghose 1987), HPLC, YSI 2700 SELECT, OneTouch Ultra, and Ascensia Contour. In DNS assay, the 3,5-dinitrosalicylic acid is reduced to produce a colour change, which was measured at 540 nm. Waters Sugar-Pak was used as HPLC columns with Waters refractometer R401 and 501 HPLC Pump for the STB experiment. Distilled and deionized water was used as the mobile phase. The operating flow rate was 0.5 ml/min; the retention time was 8.5 min and was operated at 90°C. The filtered medium was filtered again with a membrane filter (0.45 μm, Millipore, USA) before injection.

OneTouch Ultra and Ascensia Contour test strips were purchased from a local pharmacy. OneTouch uses GOx enzyme with ferricyanide as the mediator. The glucose detection range is from 0.2 to 6 g/L with a sample size of 1 μL. Ascensia uses a PQQ-GDH enzyme with a potassium ferricyanide as the mediator. The range is between 0.1 to 6 g/L with a sample size of 0.6 μL. Samples tested with the glucose monitors were read in triplicates. OneTouch requires coding, where the code on the vial of test strips must match the one on the monitor. This code is used for calibrating the meter with the strips, which is dependent on the manufacturers' lot. Ascensia does not require coding, which is achieved by tighter quality control when manufacturing the strips (Newman and Turner 2005).

Results and Discussions

Glucose solutions

The results of the glucose concentration measurements using both meters are shown in Figures 3.1 and 3.2 and in Table 3.2. Both meters gave a good correlation for glucose in water solutions in the range of 0.5 to 4 g/L. Above 4 g/L, OneTouch gives a non linear response and Ascensia showed a plateau which makes it difficult to determine the glucose concentration above 4 g/L. The pH of the solution had a larger effect on the measurements

with the OneTouch meter than with the Ascensia meter. The glucose solutions at pH 4.6 were tested with a different lot of strips for OneTouch and the regression lines obtained for both lots are shown in Table 3.2. Statistical F-test and t-test showed respectively that the variances and the means for both lots were not significantly different with a 95% confidence level.

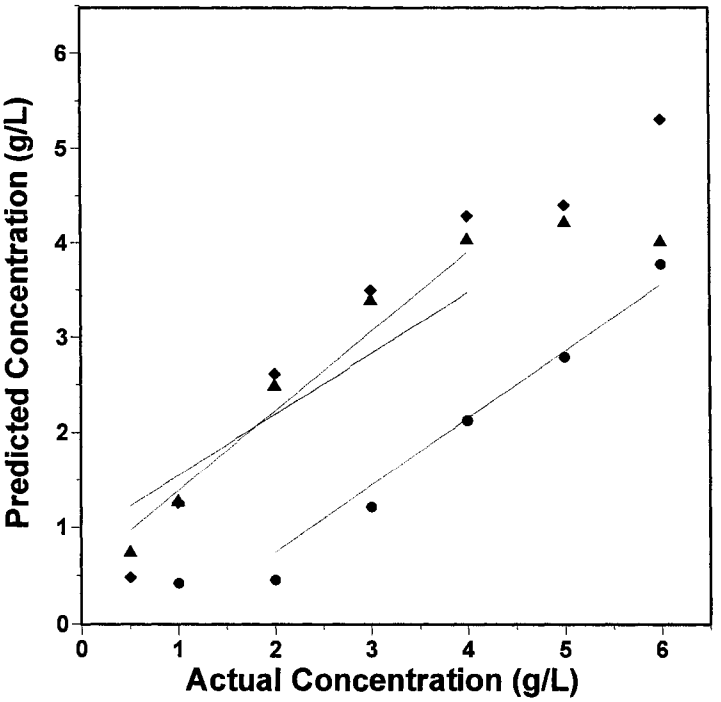

Figure 3.1. Comparison of displayed OneTouch and actual glucose concentration in: water at pH 4.6(▲); water at pH 8.6 (◆), and growth medium (●).

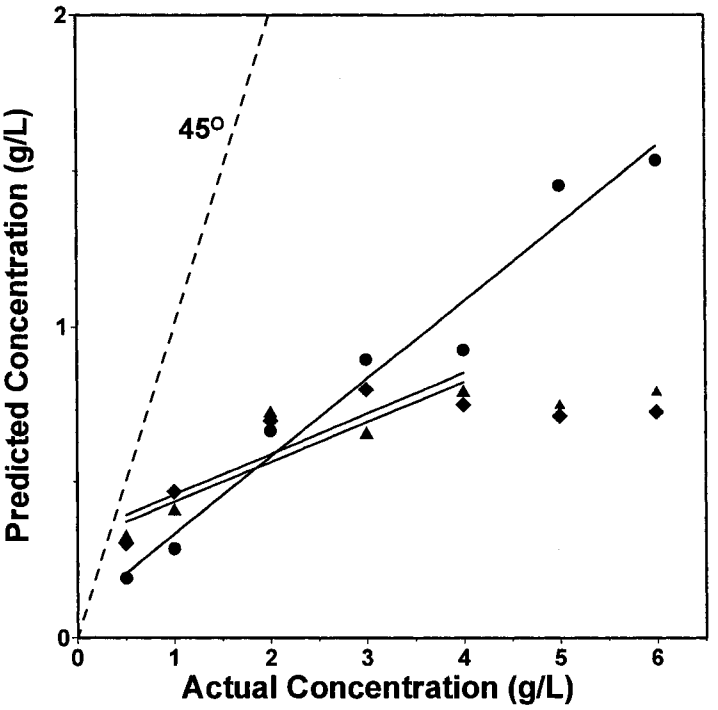

Figure 3.2. Comparison of displayed Ascensia and actual glucose concentration in: water at pH 4.6(▲); water at pH 8.6 (◆), and growth medium (●).

In the growth medium, Ascensia was able to achieve a linear response between 0.5 to 6 g/L whereas for the OneTouch meter the linear range was between 2 to 6 g/L of the actual concentration. Concentration below 0.5 g/L resulted in an error for OneTouch. From Table 2.2, the standard deviation of the displayed measurements by OneTouch is smaller in the growth medium than in the aqueous glucose solutions while Ascensia showed the opposite trend. The effective linear range of both meters is wider for the growth medium than for the aqueous glucose solutions.

Ascensia Contour gave values that were significantly lower than the actual concentrations, and the effective linear range was much smaller than for the OneTouch. For later experiments, samples were diluted to insure that the actual glucose concentration in the analyzed samples was below 4 g/L, corresponding to the linear region of both meters.

Table 3.2. Regression models for predicting actual glucose concentration (C_A) versus displayed glucose concentration (C_D) using blood glucose monitors.

Solutions	OneTouch Ultra	Ascensia Contour
Aqueous glucose solution pH 4.6	Lot 1: $C_A = 1.0403C_D - 0.3741$ $R^2 = 0.986$ Lot 2: $C_A = 1.1667C_D - 0.0599$ $R^2 = 0.985$ $\sigma = 0.21$	$C_A = 7.7761C_D + 2.3787$ $R^2 = 0.8137$ $\sigma = 0.09$
Aqueous glucose solution pH 8.6	$C_A = 0.9260C_D - 0.1458$ $R^2 = 0.981$ $\sigma = 0.29$	$C_A = 7.7645C_D + 2.4969$ $R^2 = 0.7914$ $\sigma = 0.12$
Growth medium pH 4.8	$C_A = 1.2192C_D + 1.4762$ $R^2 = 0.9973$ $\sigma = 0.18$	$C_A = 4.0016C_D + 0.3245$ $R^2 = 0.9664$ $\sigma = 0.20$

Flasks fermentations

Initial flask fermentations were performed to test the suitability of the glucose analyzer in the presence of medium, microorganisms and products. Both meters gave a linear response in the range of 0.5 to 4 g glucose/L as determined by DNS and YSI. The results obtained were compared to the average concentration obtained by DNS and YSI as shown in Figure 3.3. The concentrations of glucose obtained by the Ascensia meter were lower than the actual values while those obtained by OneTouch were higher. However, correcting the values with the regression line obtained with the initial growth medium (Table 3.2) will result in overestimating the actual concentration for both meters. The most probable reason for this difference could be due to metabolites produced during fermentation. Therefore, the correlation obtained from this experiment was used later to obtain glucose concentration during the experiments performed in STB.

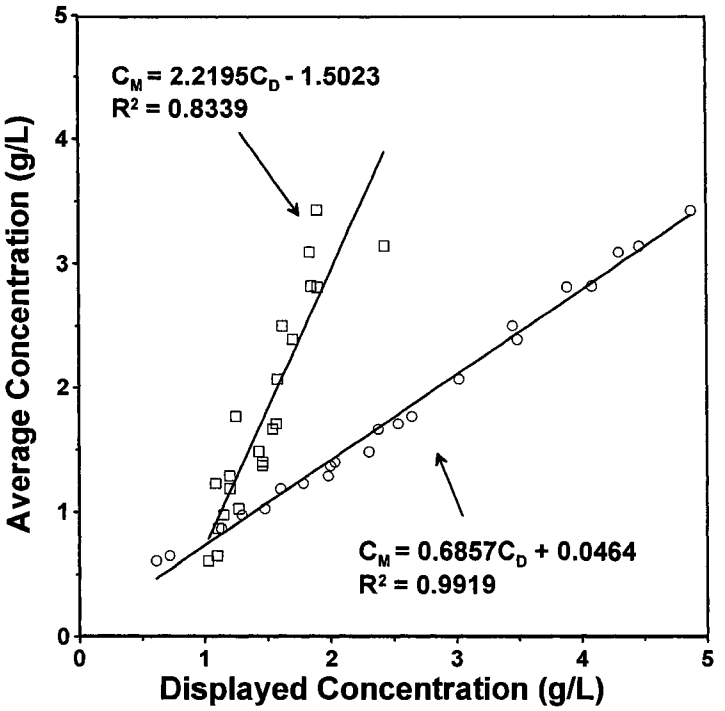

Figure 3.3. Comparison of glucose concentration displayed (C_D) on OneTouch (○), Ascensia (□) and average measured (C_M) by DNS and YSI for flask experiments.

Experiment in STB

A STB experiment was performed and the results are shown in Figure 3.4. It shows that the glucose consumption corresponds very well to the growth curve. Also, the glucose monitors showed a good estimate of glucose concentration similar to other methods when corrected with the corresponding calibration curves shown in Figure 3.3. The average standard deviation of the displayed measurements for OneTouch was 0.044 g/L whereas it was 0.16 g/L for Ascensia. OneTouch shows a lower standard deviation for the fermentation medium than for glucose solutions.

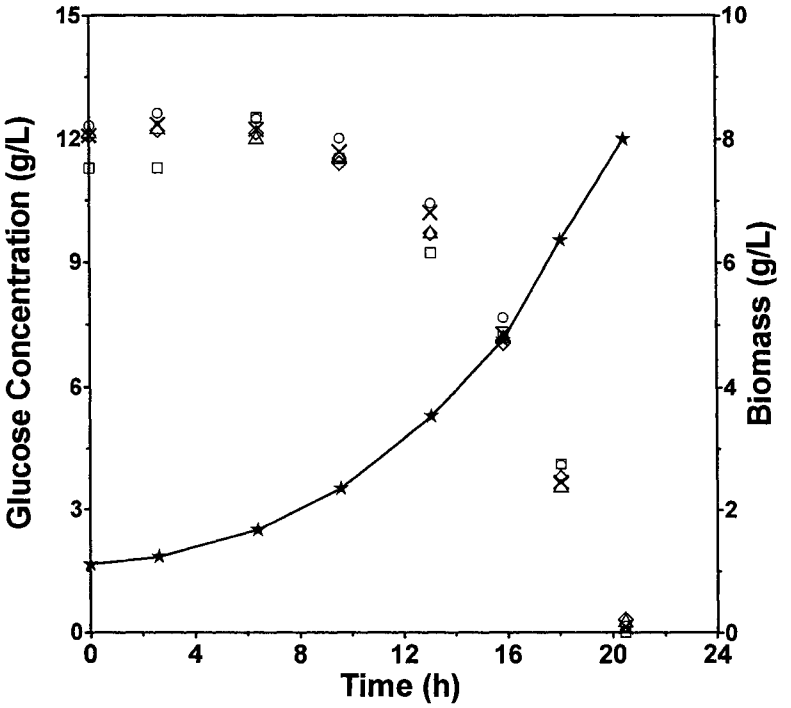

Figure 3.4. Evolution of biomass (★) and glucose concentration measured by YSI (◊), HPLC (Δ), DNS (×), OneTouch (○), and Ascensia (□) for STB runs.

Different lots of OneTouch strips were used for the flasks and STB experiment. The calibration curve obtained earlier continued to give a very good correlation, indicating there is no need to calibrate for each new lot of strips. Similarly, three different lots of Ascensia strips were used. Even though the Ascensia meter displayed a smaller effective range of glucose, good results were achieved. The presence of fermentation products and metabolites as observed from HPLC results did not appear to interfere significantly with either glucose meters.

Conclusion

Both OneTouch and Ascensia glucose monitors gave results similar to HPLC, DNS and YSI for estimating the glucose concentration when corrected with the calibration obtained from actual fermentation experiments. It is therefore suggested to calibrate the meters using actual fermentation samples. The effect of pH is eliminated by adding citrate

buffer into the filtered samples. For both meters, there is no significant difference between various lots of measurement strips. The time and cost benefits are major advantages of these meters. However, different medium could respond differently to the enzyme used in the test strips for the meters and one must test and decide which meter is more suitable for their application. For *Trichoderma reesei* fermentations, the OneTouch meter was chosen to be more suitable due to its larger effective linear range and lower standard deviation.

Acknowledgment

The authors would like to thank Dr. J. Zhang at the Department of Chemical Engineering, University of Ottawa for lending the YSI 2700 SELECT biochemistry analyzer. The authors also thank Iogen Corporation for providing the *Trichoderma reesei* RUT C-30 strain. The financial contribution of the Natural Science and Engineering Research Council (NSERC) is acknowledged.

References

Cook RM., Devlin BR, Ebeler SE, Butzke CE (1998) Evaluation of a digital blood glucose monitor for measuring residual glucose in wine. Am. J. Enol. Vitic. 49:225-228.

D'Costa EJ, Higgins IJ, Turner APF (1986) Quinoprotein glucose dehydrogenase and its application in an amperometric glucose sensor. Biosensors. 2:71-87.

FitzGerald J, Vermerris W (2005) The utility of blood glucose meters in biotechnological applications. Biotechnol. Appl. Biochem. 41: 233-239.

Ghose TK (1987) Measurement of Cellulase Activities, Pure & Appl. Chem. 59:257-268.

Lee J, Lee SY, Park S, Middelberg APJ (1999) Control of fed-batch fermentations. Biotechnol. Adv. 17:29–48.

Iversen M, Finstad B, McKinley RS, Eliassen RA (2003) The efficacy of metomidate, clove oil, Aqui-S™ and Benzoak® as anaesthetics in Atlantic salmon (*Salmo salar* L.) smolts, and their potential stress-reducing capacity. Aquaculture. 221:549-566.

Iversen M, Finstad B, McKinley RS, Eliassen RA, Carlsen KT, Evjen T (2005) Stress responses in Atlantic salmon (*Salmo salar* L.) smolts during commercial well boat transports, and effects on survival after transfer to sea. Aquaculture. 243:373-382.

Minihane BJ, Brown DE (1986) Fed-batch culture technology. Biotechnol. Adv. 4:207–218.

Nayak RC, Herman IR (1997) Measurement of glucose consumption by hybridoma cells growing in hollow fiber cartridge bioreactors: use of glucose self-monitoring devices. J. Immunol. Meth.. 205:109-114.

Newman JD, Turner Anthony PF (2005) Home blood glucose biosensors: a commercial perspective. Biosens. Bioelectron.. 20:2436-2453.

Tang Z, Louie RF, Lee JH, Lee DM, Miller EE, Kost GJ (2001) Oxygen effects on glucose meter measurements with glucose dehydrogenase-and oxidase-based test strips for point-of-care testing. Crit. Care Med. 29:1062-1070.

Weibel MK, Bright HJ (1971) The Glucose Oxidase Mechanism. Interpretation of the pH dependence. J. of Biological Chem. 246:2734-2744.

Chapter 4
Conclusion

The effect of agitation on the morphology of *T. reesei* was studied with the aid of image analysis. Eight fermentations were performed, four in STB and four in RPB, at various agitation speeds. It was found that during the fedbatch phase, neither the type of mixing devices nor the speed of agitation had an affect on the area and perimeter of each of the four morphological types. Higher agitations in both STB and RPB resulted in a higher growth rate and higher amount of fragmentation which began at the end of the batch phase when substrate concentration was low. Protein production began at the end of the batch phase and lactose was fed during the fedbatch phase to induce cellulase production. A maximum protein concentration of 3 g/L was obtained at the end of the fermentations, and the protein productivity was very low, less than 0.13 IU/mL h for all runs.

T. reesei grown in the STB was able to achieve a higher productivity, with the highest productivity at 400 RPM. A correlation between the morphological parameter, HGU, and protein production was also found. High shear (i.e. 500 RPM in STB) was shown to be detrimental to the microorganisms. There was a higher amount of fragmentation which resulted in more dead tips that did not produce proteins. Thus, to obtain an optimal protein production, the STB should be operated at 400 RPM and the RPB at 1.0 Hz.

A quick and economical method for measuring glucose concentration during a fungal fermentation by using home blood glucose monitors was developed. OneTouch meter was found to be more suitable for the fungal fermentation of *T. reesei.* Since these blood glucose meters are calibrated with glucose solution similar to blood, they will need to be recalibrated with actual fermentation samples. Lot to lot differences of the strips were found to be insignificant hence there is no need to recalibrate for each new lot of strips, and the effect of pH is eliminated by adding citrate buffer to the samples being tested.

Appendix A

List of measured morphological parameters

Various morphological parameters were measured with the Image Analysis VB subroutines that were written by Lecault et al. (2007) and embedded in the software ImagePro Plus. However, some of the parameters were not studied in depth. The list of parameters that were measured for each morphological class (Figure A.1) is presented in Table A.1 and the definitions are listed in Table A.2.

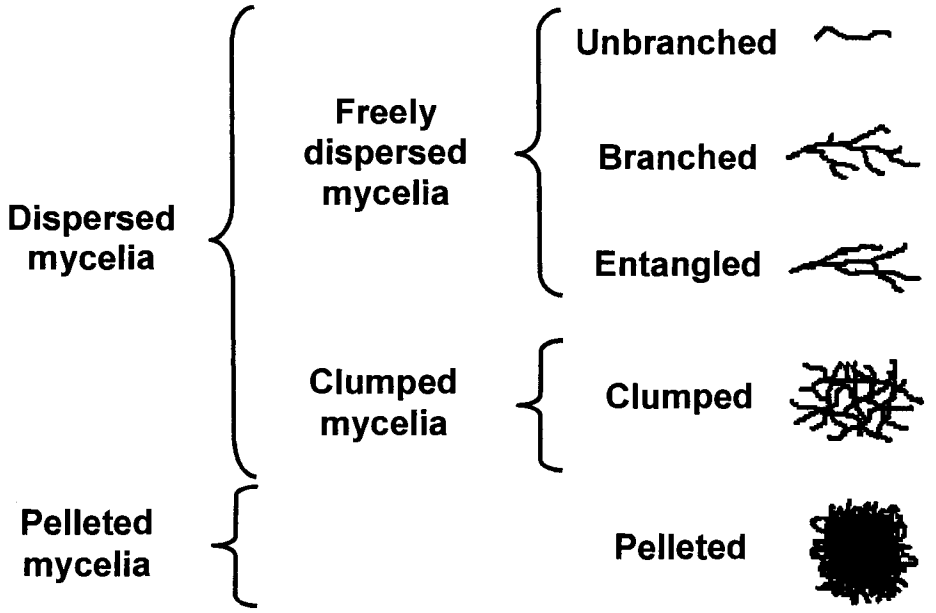

Figure A.1. Schematic representation of the morphological classification for filamentous species.

Table A.1. Measured morphological parameters for each morphological type.

Unbranched	Branched	Entangled	Clumped
Area	Area	Area	Area
Box/area ratio	Box/area	Box/area ratio	Box/area ratio
Aspect Ratio	Aspect Ratio	Aspect Ratio	Aspect Ratio
Perimeter	Perimeter	Perimeter	Perimeter
Convex Perimeter	Convex Perimeter	Convex Perimeter	Convex Perimeter

Perimeter Ratio	Perimeter Ratio	Perimeter Ratio	Perimeter Ratio
Roundness	Roundness	Roundness	Roundness
Fractal Number	Fractal Number	Fractal Number	Fractal Number
Dendritic length	Fullness	Fullness	Fullness
Viable Area	Dendritic length	Number of Holes	Number of Holes
Mean Diameter	Number of tips	Dendritic length	Dendritic length
% viability	Minimum branch length	Number of tips	Number of tips
Sum Density	Maximum branch length	Minimum branch length	Minimum branch length
	Mean branch length	Maximum branch length	Maximum branch length
	Number of internodal units	Mean branch length	Mean branch length
	Minimum internodal length	Number of internodal units	Number of internodal units
	Maximum internodal length	Minimum internodal length	Minimum internodal length
	Mean internodal length	Maximum internodal length	Maximum internodal length
	Branching Order	Mean internodal length	Mean internodal length
	Viable Area	Viable Area	Viable Area
	Mean Diameter	Mean Diameter	Mean Diameter
	HGU length	HGU length	HGU length
	HGU volume	HGU volume	HGU volume
	% viability	% viability	% viability
	Sum Density	Sum Density	Sum Density

Table A.2. Definitions of the morphological parameters

Morphological Parameters	Definitions
Area	Projected area of the microorganism excluding holes. It can have units of pixels or μm^2 for calibrated images.
Aspect ratio	Ratio between the major and minor axes of an ellipse equivalent to the object.
Area/box ratio	Ratio between the area of an object (excluding holes) and its bounding box. This parameter refers to the compactness of the microorganism.
Branch length	Length of an individual branch.
Convex perimeter	Perimeter obtained by measuring the convex outline of the object.
Diameter	Hyphal diameter obtained by dividing the area by the total length
Fractal Number	Fractal dimension of the object's outline.
Fullness	Ratio of the area of the object excluding holes to the area of the object including holes.
HGU length	Total length divided by the number of tips.
HGU volume	Total volume divided by the number of tips. The shape of the mycelia is assumed to be a cylinder and the HGU volume is calculated as follow : $$\text{HGU volume} = \frac{\pi \times Diameter \times Area}{4 \times \text{ number of tips}}$$
Internodal distance	Length of an individual segment between two branching points.
Percentage of viability	Ratio of the viable area to the total area.
Perimeter	Length of the outline of the microorganism.
Perimeter ratio	Ratio of the convex perimeter to the perimeter.
Roundness	Shape factor describing the deviation of object from being perfectly circular. The roundness is calculated as follow : $$\text{Roundness} = \frac{\text{Perimeter}^2}{4\pi\text{Area}}$$ A true circle has a circularity of 1 whereas a non circular object has a greater value.
Number of holes	Number of compartments showing the background within the area of an object. Holes are usually formed by entanglement and overlapping of mycelia.
Number of tips	Number of end points on the skeleton of the mycelia.
Sum Density	The sum of the intensity values of all the pixels of a counted object

Total length	Total length of the skeleton. This parameter includes all the branch lengths and the internodal lengths.
Viable area	Area of parts of the microorganisms having enzymatic activity and intact membrane.
Viability	Dividing the viable area by the total area of the microorganism.

Appendix B

Statistical Validation 1

Statistical validation was performed with several morphological parameters to determine the appropriate number of sets of pictures required for image analysis in order to accurately represent the microorganism population. Firstly, the mean value of the morphological parameter is plotted against the increasing number of images analysed and 60 images was found to be sufficient. Secondly, 60 images were selected randomly 100 times from a large set of captured images. The results shown here are obtained from 2 different fermentation runs in the STB and at different phases.

The following are the results obtained during the batch phase and 100 sets of images were captured. The time required to acquire these 100 sets of pictures was 60 minutes. The number of hyphal objects analyzed on each slide ranged from 2-3 objects. The average number of hyphal objects per frame was 2. From Figures B.1 and B.2, it can be seen that the diameter and HGU began to stabilize at approximately 60 images at 4.41 μm and 52 μm/tips, respectively. When 60 images were chosen randomly 100 times out of the 100 sets of images, the standard deviation was very small (Table B.1).

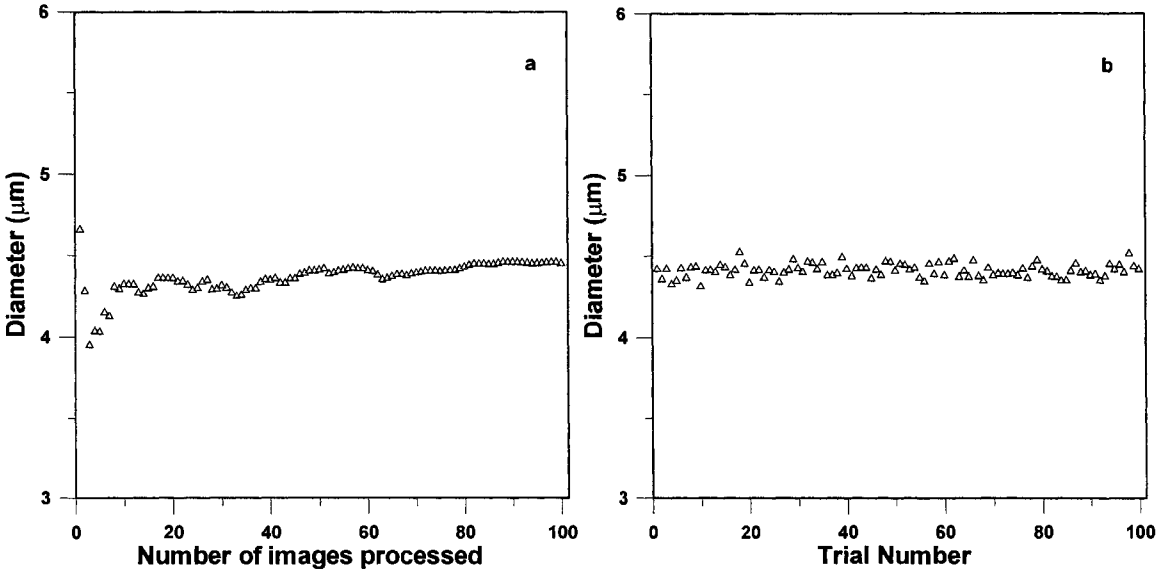

Figure B.1. Mean hyphal diameter (a) of the free mycelia with respect to the number of sequential images analyzed and (b) when 60 images amongst the 100 were randomly selected.

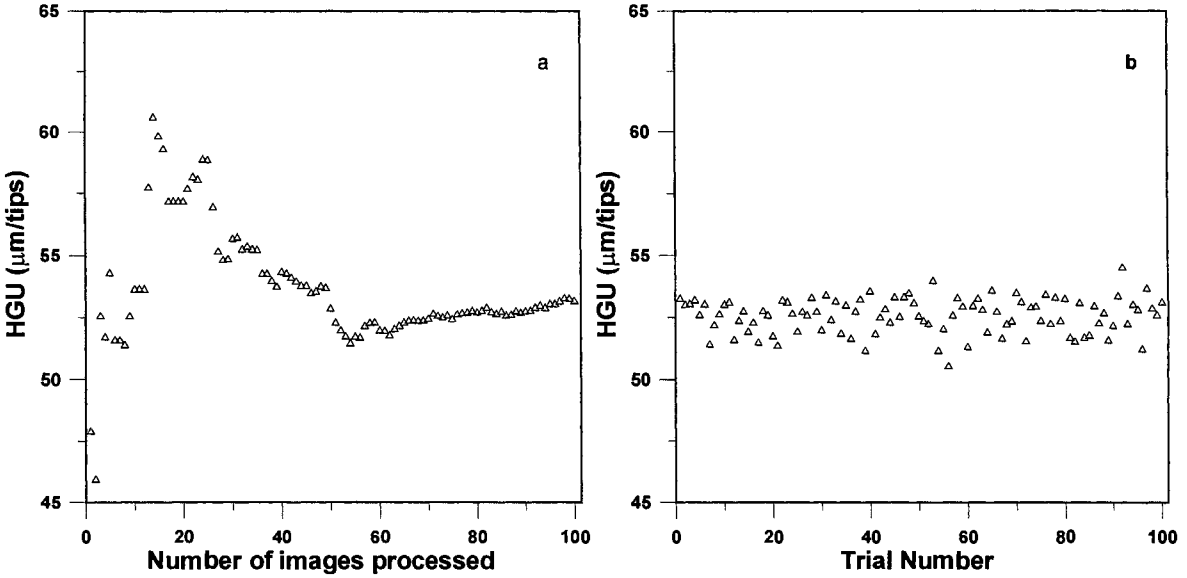

Figure B.2. Mean hyphal growth unit of *T. reesei* (a) with respect to the number of sequential images analyzed and (b) when 60 images amongst the 100 were randomly selected.

Table B.1. The mean value morphological parameters when 60 images were chosen randomly 100 times from the set of 100 images.

Parameter	Mean value
Diameter (μm)	4.41 ± 0.04
HGU (μm/tips)	52.60 ± 0.72

At the end of the batch phase for the fermentation performed in the STB at 200RPM, a set 220 of frames were captured to perform an additional validation of the results. The time required to acquire these 220 frames was less than 120 minutes and required 3 slides. The average number of hyphal objects analyzed on each frame ranged from 2-3 objects. In Figure B.3., only the first 91 images, corresponding to the first slide, were analyzed sequentially. The sample was taken at 37 h from STB at 400 RPM at the end of its batch phase when there is a higher amount of clumps in the bioreactor. It was observed visually that the amount of clumps was higher on one side of the slide; hence the area fractions did not converge to a constant value and showing a slight declining trend as more images were analyzed. Also, the sudden increase followed by a decrease when fewer images are analyzed is due to the appearance of large clumps which caused large increase. Due to the distribution of the microorganisms, it is important to acquire the images across the entire slide. It can be seen that after 60 images, the area of fraction of clumps decreases and branched increases. To compromise between accuracy, time, and storage space, 60 images were deemed as sufficient. At 60 images, the area fractions are as follows: unbranched, 0.020; branched, 0.203; entangled, 0.236; and clumped, 0.541. When 60 images were chosen 100 times randomly out of the set of 100 of images (Figure B.4), the variation was about 20%. The diameter (Figure B.5a) and HGU (Figure B.6a) showed similar results and the mean value was 4.11 μm and 41.95 μm/tips, respectively at 60 images.

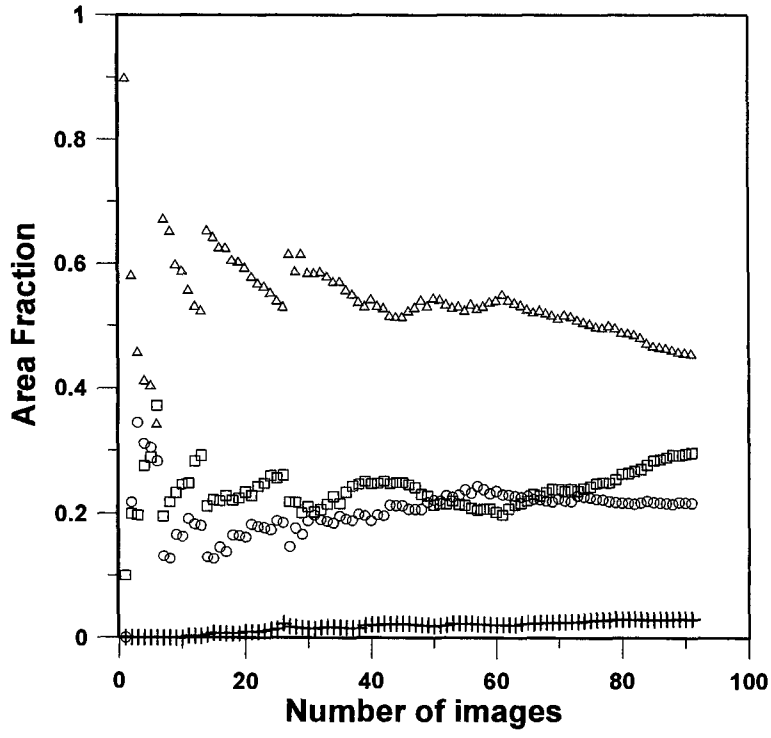

Figure B.3. Area fractions of unbranched (+), branched (□), entangled (O) and clumped (Δ) morphologies with respect to the number of sequential images analyzed that were captured in the first slide. Sample taken at 37 h for the fermentation performed in STB at 400 RPM.

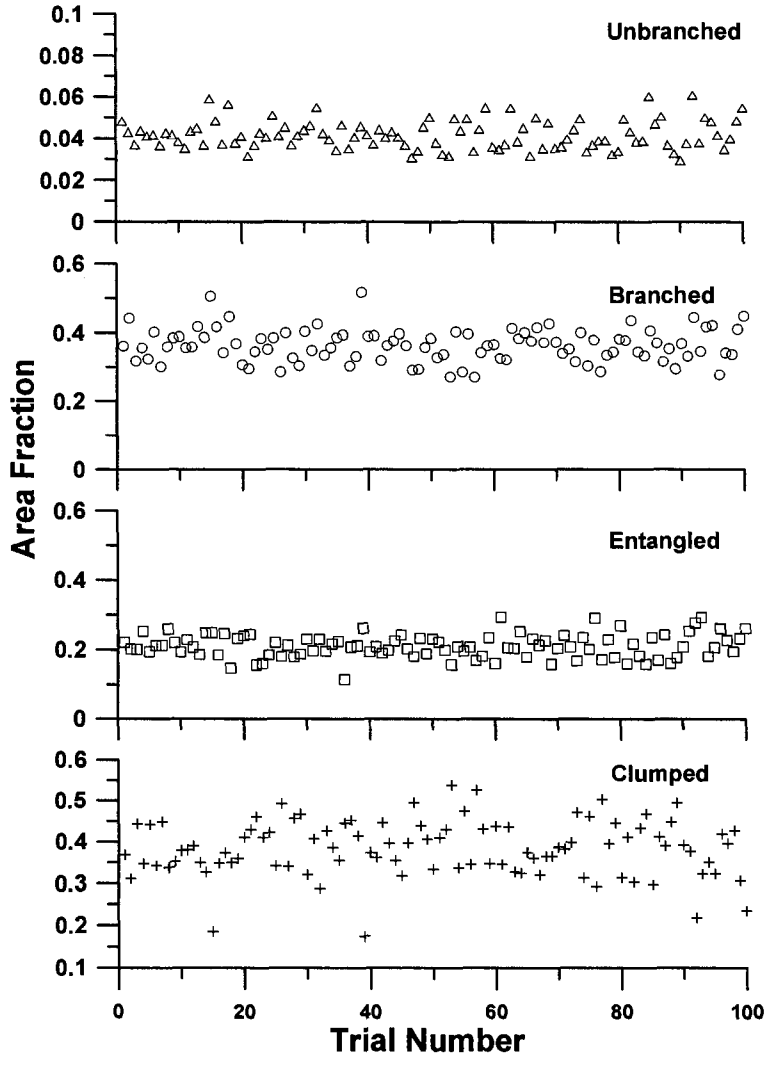

Figure B.4. Variation of area fraction of each morphological type, unbranched (+), branched (□), entangled (O) and clumped (Δ) when 60 images amongst the 220 were randomly selected.

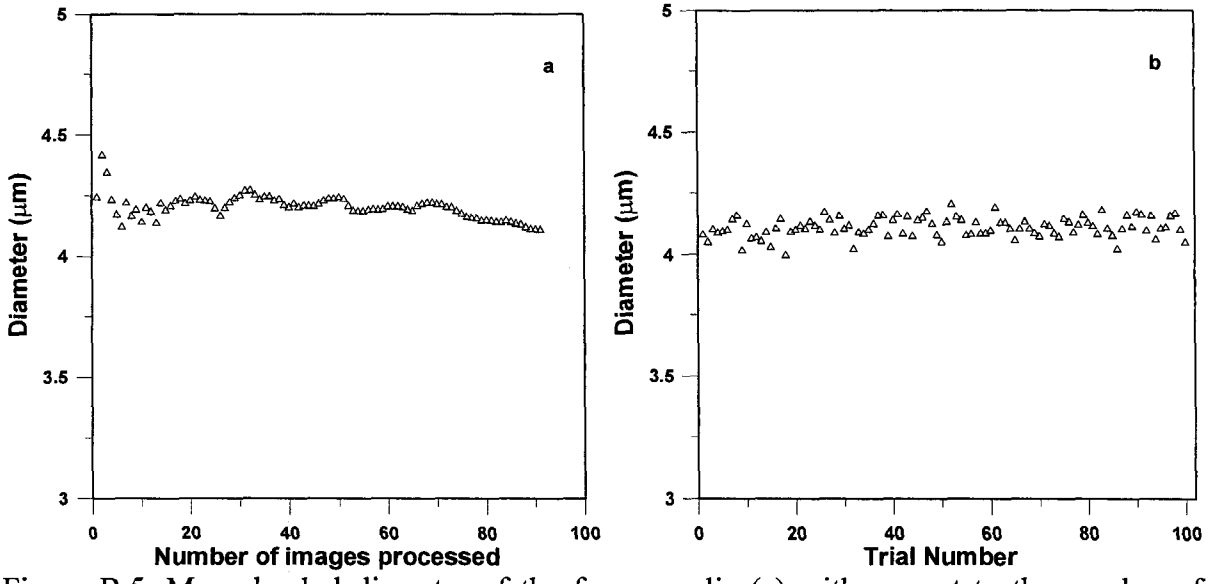

Figure B.5. Mean hyphal diameter of the free mycelia (a) with respect to the number of sequential images analyzed and (b) when 60 images amongst the 220 were randomly selected.

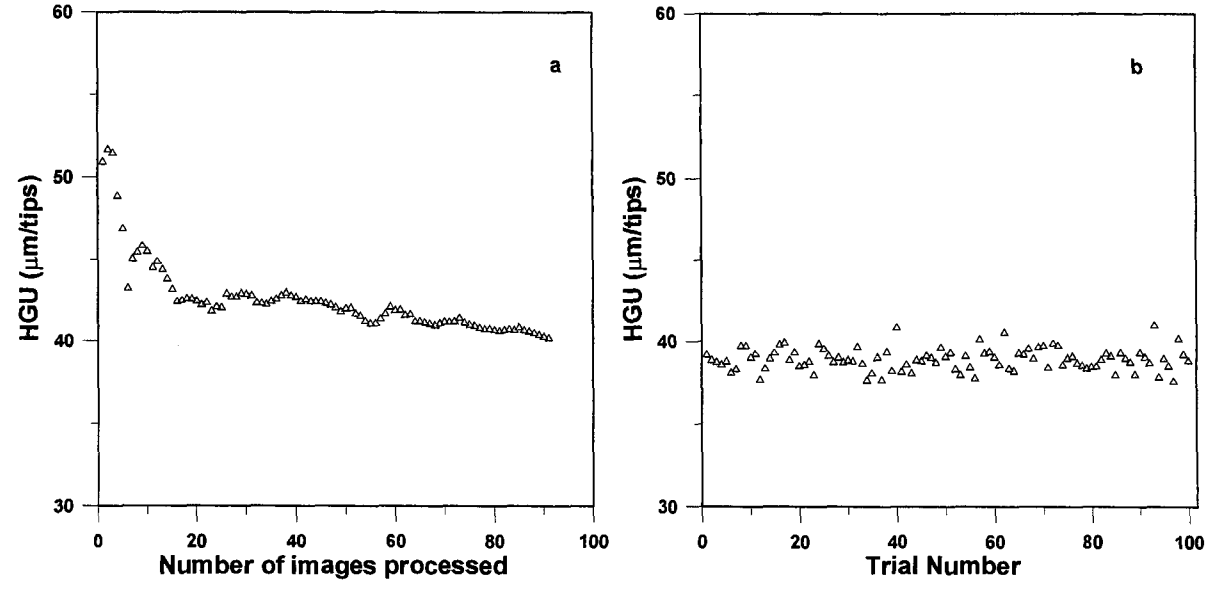

Figure B.6. Mean hyphal growth unit of *T. reesei* (a) with respect to the number of sequential images analyzed and (b) when 60 images amongst the 220 were randomly selected.

Table B.2. The mean value of morphological parameters when 60 images were chosen randomly 100 times from the set of 220 images.

Parameters	Mean value
Unbranched	0.042 ± 0.007
Branched	0.364 ± 0.048
Entangled	0.211 ± 0.034
Clumped	0.389 ± 0.067
Diameter (μm)	4.11 ± 0.04
HGU (μm/tips)	38.98 ± 3.87

From the analysis, 60 images are sufficient to determine the mean value of different morphological parameters with a mean number of 2-3 hyphal objects per image.

Appendix C

Statistical Validation 2

A nested hierarchical design was conducted at two different times in the STB at 400 RPM: the first time during the batch phase, and the second time during the fedbatch phase. The sampling procedure was described in Chapter 2.

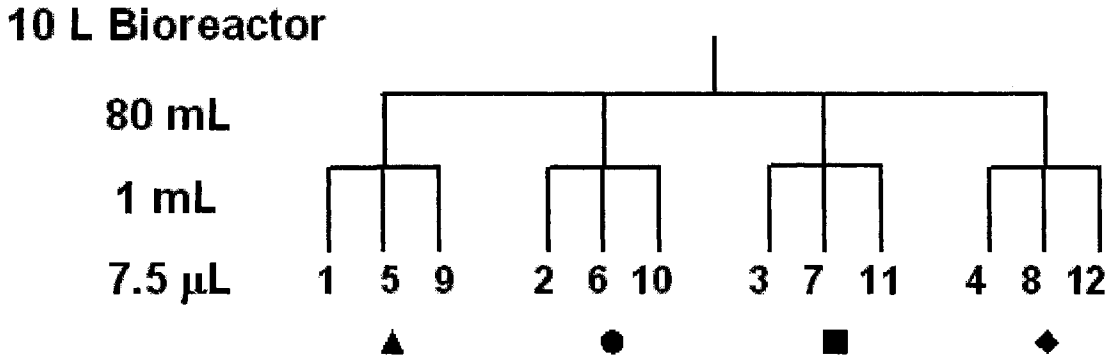

Figure C.1. Sampling sequence for the 2 x 2 x 3 hierarchical design for estimating the components of the variance. The numbers at the third level indicates the sequence images were acquired.

The results obtained during the batch phase at 16 h are presented in the following section. The image acquisition of the 12 sets of images required a total of 6 h. The number of hyphal objects analyzed for each set of images ranged from 90-130 objects. From Figures C.2 and C.3, the time at which the image was captured did not have an effect on the HGU or the diameter parameter, and the largest variance occurred on the slide (Tables C.1 and C.2). As explained in Chapter 2, the negative variance can be assumed to be zero or negligible as it is very small.

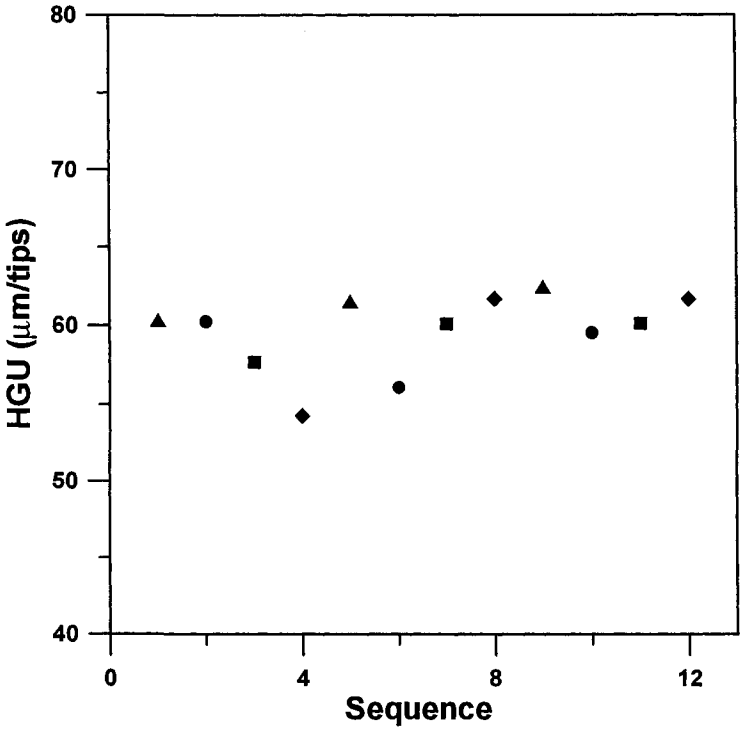

Figure C.2. HGU for each of the 12 sets of images taken at 16 h for the fermentation performed at 400 RPM in the STB.

Table C.1. ANOVA of the HGU for the 12 sets of images of taken at 16 h for the fermentation performed at 400 RPM in the STB.

Source of Variation	Sum of squares	Degrees of freedom	Mean square	Variance
Average	42660	1		
1st Level	1.829	1	1.829	-1.800
2nd Level	11.987	2	5.993	-0.215
3rd Level	53.103	8	6.638	6.638
Total	42726	12		

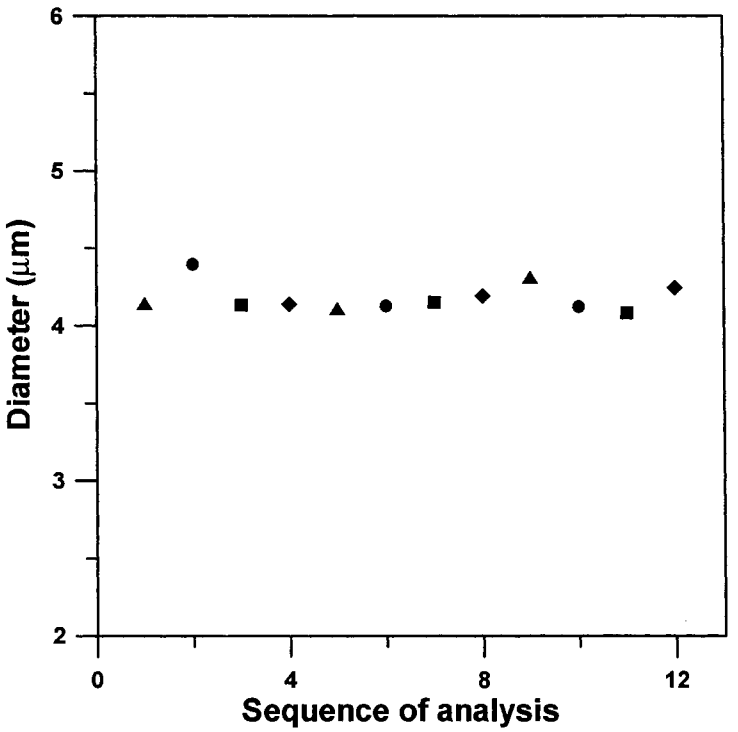

Figure C.3. Diameter for each of the 12 sets of images taken at 16 h for the fermentation performed at 400 RPM in the STB.

Table C.2. ANOVA of the diameter for the 12 sets of taken at 16 h for the fermentation performed at 400 RPM in the STB.

Source of Variation	Sum of squares	Degrees of freedom	Mean square	Variance
Average	209.702	1		
1st Level	0.006	1	0.006	-0.001
2nd Level	0.008	2	0.004	-0.002
3rd Level	0.079	8	0.010	0.010
Total	209.796	12		

Figures C.4 and C.5 present the clump and branched area fractions of the 12 samples taken during the batch phase. There was no effect of time of capture on the area fraction of both types of morphology.

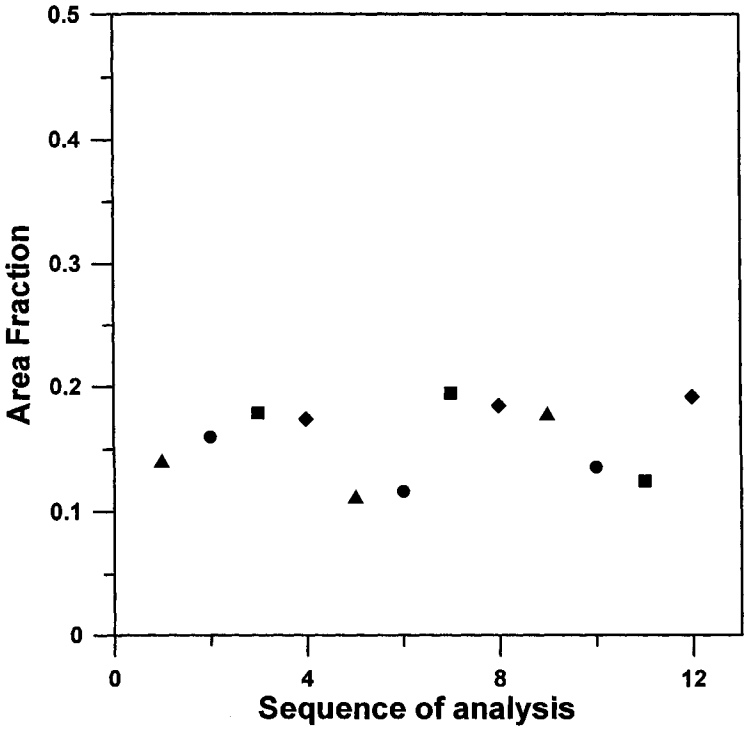

Figure C.4. Branched area fraction for each of the 12 sets of taken at 16 h for the fermentation performed at 400 RPM in the STB.

Table C.3. ANOVA of the branched area fraction for the 12 sets of images taken at 16 h for the fermentation performed at 400 RPM in the STB.

Source of Variation	Sum of squares	Degrees of freedom	Mean square	Variance
Average	0.297	1		
1st Level	0.004	1	0.004	0.0004
2nd Level	0.001	2	0.000	-0.0002
3rd Level	0.006	8	0.001	0.0008
Total	0.307	12		

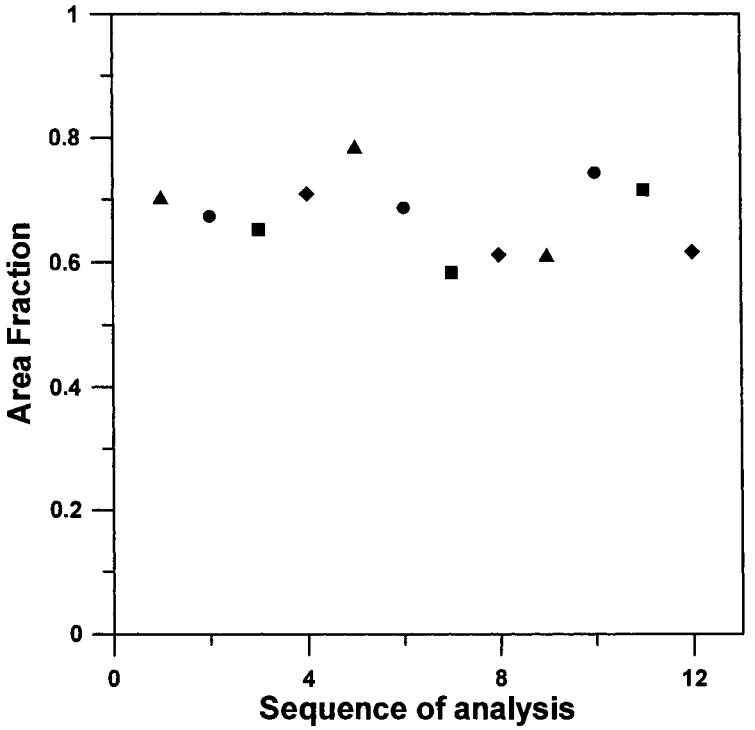

Figure C.5. Clumped area fraction for each of the 12 sets of images taken at 16 h for the fermentation performed at 400 RPM in the STB.

Table C.4. ANOVA of the clumped area fraction for the 12 sets of images for taken at 16 h for the fermentation performed at 400 RPM in the STB.

Source of Variation	Sum of squares	Degrees of freedom	Mean square	Variance
Average	5.449	1		
1st Level	0.008	1	0.008	0.0007
2nd Level	0.000	2	0.000	-0.0014
3rd Level	0.033	8	0.004	0.0041
Total	5.490	12		

Results obtained during the fedbatch phase at 60 h in the STB at 400 RPM are now examined. The image acquisition of the 12 sets of images required a total of 6 h. The number of hyphal objects analyzed for each set of images ranged from 200 to 367 objects.

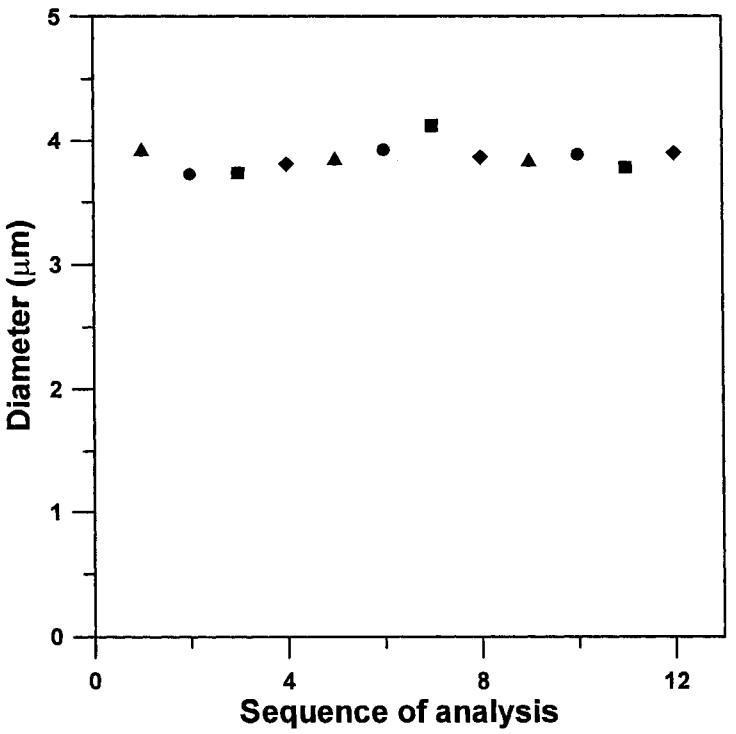

Figure C.6. Diameter for each of the 12 sets of images taken at 60 h for the fermentation performed at 400 RPM in the STB.

Table C.5. ANOVA of the diameter for the 12 sets of images taken at 60 h for the fermentation performed at 400 RPM in the STB.

Source of Variation	Sum of squares	Degrees of freedom	Mean square	Variance
Average	179.317	1		
1st Level	0.000	1	0.000	-0.003
2nd Level	0.002	2	0.001	-0.005
3rd Level	0.120	8	0.015	0.015
Total	179.439	12		

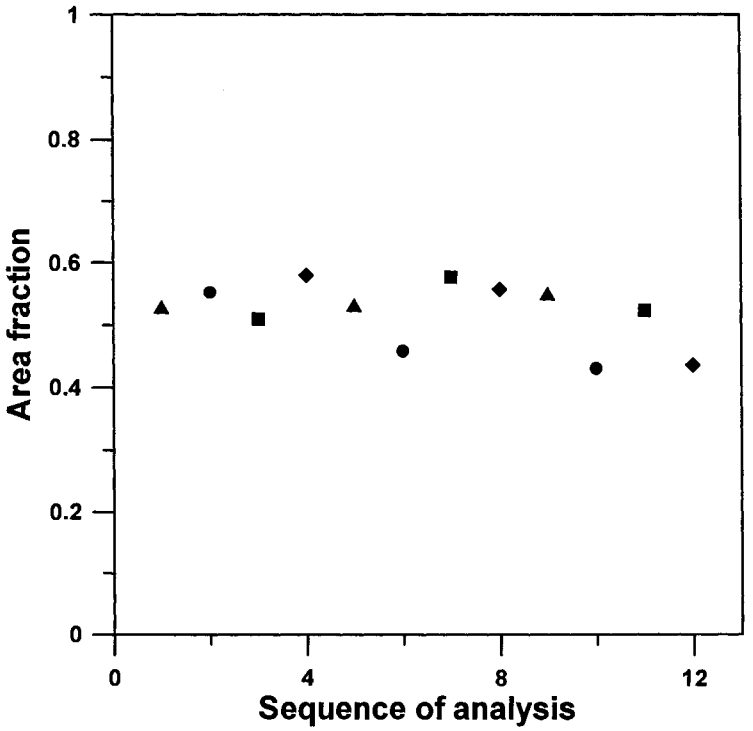

Figure C.7. Branched area fraction for each of the 12 sets of images taken at 60 h for the fermentation performed at 400 RPM in the STB.

Table C.6. ANOVA of the branched area fraction for the 12 sets of images taken at 60 h for the fermentation performed at 400 RPM in the STB.

Source of Variation	Sum of squares	Degrees of freedom	Mean square	Variance
Average	3.233	1		
1st Level	0.001	1	0.001	-0.001
2nd Level	0.005	2	0.003	0.000
3rd Level	0.023	8	0.003	0.003
Total	3.262	12		

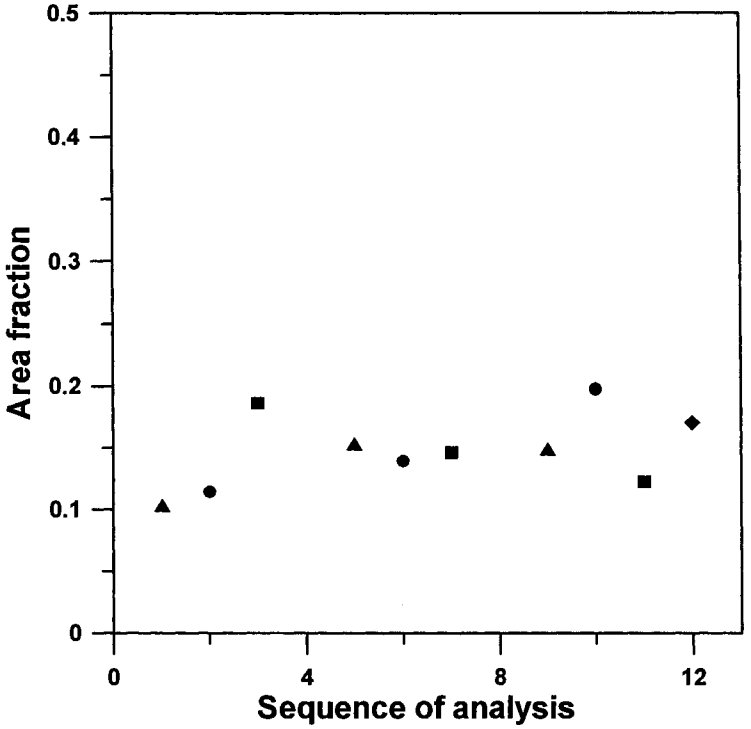

Figure C.8. Clumped area fraction for each of the 12 sets of taken at 60 h for the fermentation performed at 400 RPM in the STB.

Table C.7. ANOVA of the clumped area fraction for the 12 sets of images taken at 60 h for the fermentation performed at 400 RPM in the STB.

Source of Variation	Sum of squares	Degrees of freedom	Mean square	Variance
Average	0.261	1		
1st Level	0.000	1	0.000	0.000
2nd Level	0.000	2	0.000	0.000
3rd Level	0.010	8	0.001	0.001
Total	0.271	12		

From this study, it can be seen that the largest variation is at the 3rd level, which is due to the slide preparation and image acquisition. Also, time did not affect the diameter, HGU and area fractions of the sample. The sampling procedure from the 10 L bioreactor to the 1 mL sample introduced none to little error into the measurements.

Appendix D

Study of the influence of the magnification of the microscope on the diameter

The microscopic system is manually calibrated by acquiring an image of a calibrating slide, Stage Micrometer, at different objectives. The calibration is performed on the captured image to relate pixels with real distances. The microscope being used has 3 optical objectives with different magnifications. Images can be captured with a magnification of 10X, 20X or 40X. When images are taken with the different optical objectives, a variation in the measurement could vary depending on which optical objective was used due to possible calibration errors and the clarity of the image itself. For example, it would be harder to get a proper focus of a 3 dimensional object along the z-axis for something that was taken at a higher magnification because of the different layers and the edge could sometimes appear blurry. A test was carried out by taking a picture of a pulp filament with each of the 3 different optical objectives: 10X, 20X and 40X (Figure D.1). The diameter of the filament was taken at the circled area and was measured three times manually.

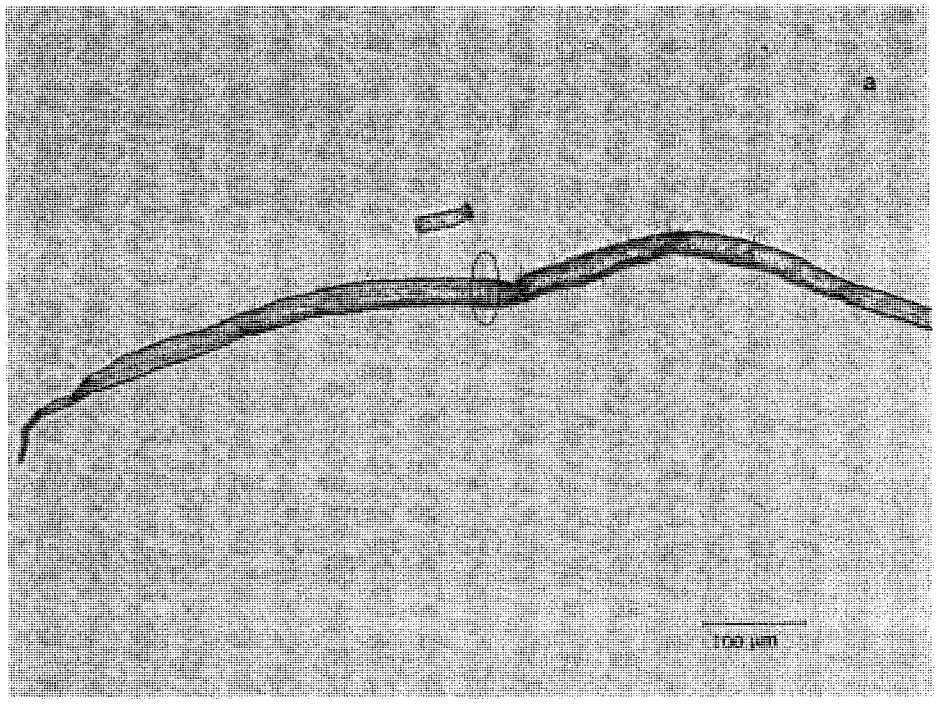

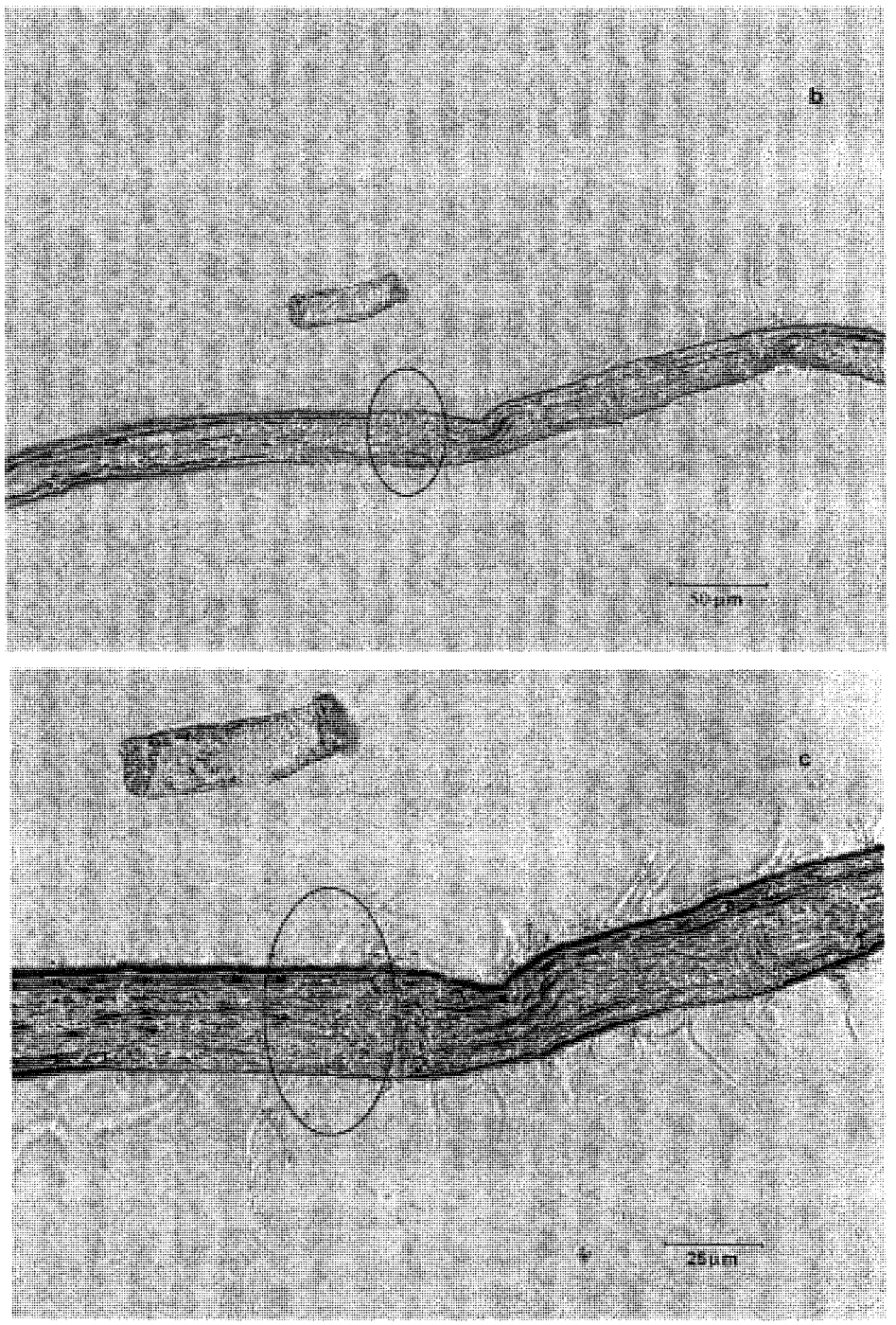

Figure D.1. Pulp filament taken under a (a) 10X, (b) 20X, and (c) 40X optical objectives.

Table D.1. The diameter of pulp measured manually with different objectives.

Measurements	10X (μm)	20X (μm)	40X (μm)
1	28.515	28.986	27.634
2	27.867	27.142	27.629
3	28.515	27.634	27.644
Mean	28.299	27.921	27.635
Standard Deviation	0.374	0.955	0.008

From Table D1., the operator error was the greatest at 20X and very minimal at 40X. The mean values shows that all measured values are almost similar and the average is 27.952 ± 0.333 μm.

Note that the diameter calculated from the image analysis subroutine was calculated by taking the area of the microorganism and dividing it by its total length. Also, all images used for image analysis were captured with a 10X optical objective for consistency.

Appendix E

Profiles of morphological parameters

This section presents the results of some of the morphological parameters that were mentioned in Appendix A. The experiments are described in Chapter 2.

The mean area as mentioned in Chapter 2 initially increases during the exponential growth phase. The area then decreases near the end of batch phase due to fragmentation caused an increase in vacuolation associated to the low substrate concentration. Figure E.1 shows the typical change in the mean area of the four morphologies. The decrease in the mean area due to fragmentation is very noticeable with the clump morphology (Figure E.1) where there is a dramatic decline in the average area when the clump is breaking down into the other 3 three types of morphology when the rate of fragmentation is higher than the rate of growth. The average area during the fedbatch phase was almost constant for the unbranched, branched and entangled morphology.

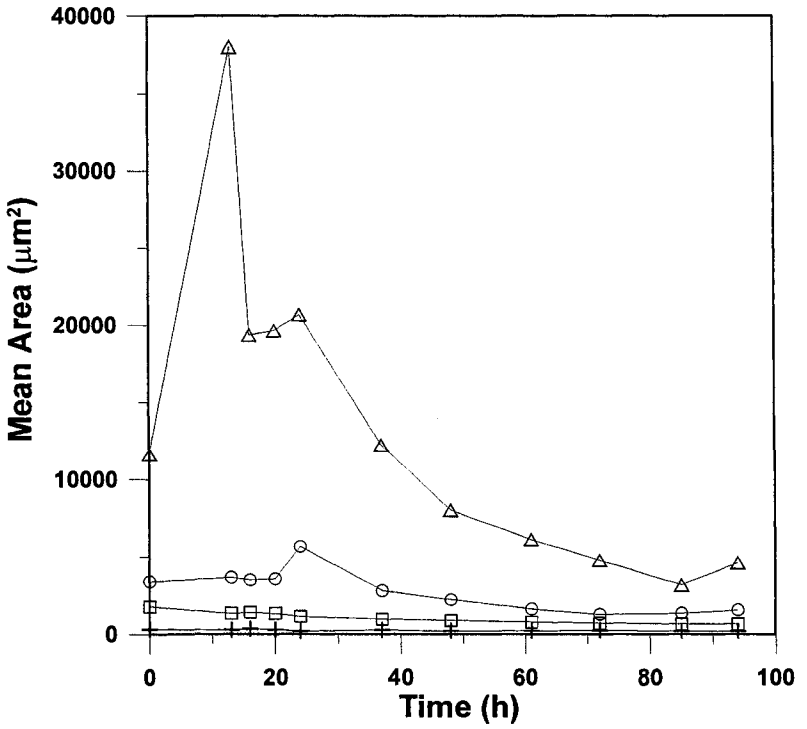

Figure E.1. Change in area of each morphological type, unbranched (+), branched (□), entangled (O) and clumped (Δ) for the fermentation in RPB at 1.0 Hz.

The distribution of the area of each morphological type (Figure A.1) during the fedbatch phase of all 8 experiments is shown in Figure E.2. As expected the unbranched morphology has the smallest area as they could be the initial spore that is germinating or they are pieces of the hyphae that was sheared from the 3 other types of morphology. Branched morphology is much larger in area, followed by entangled and clumped. The range of area of each morphological type is presented in Table 2.3.

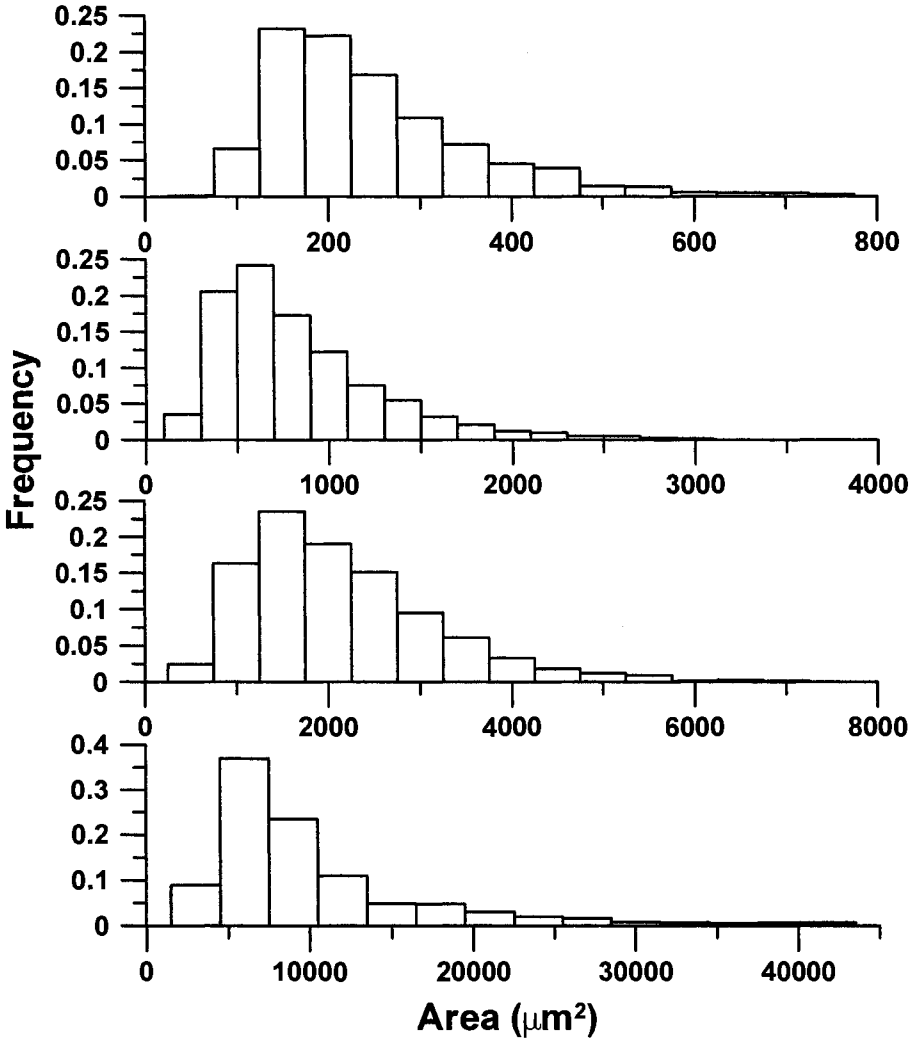

Figure E.2. Area distribution during fedbatch phase.

As mentioned in Chapter 2, the change in area fraction of each morphological type was different at the low and high agitations in both STB and RPB. Figure E.3 presents the change in area fraction of the intermediate agitation speeds in both bioreactors. In STB, at 300 and 400 RPM, the change in area fraction is similar to 500 RPM. In RPB, the change at 0.75 Hz is similar to 1.0 Hz. At 0.50 Hz, the trend lies between 0.25 and 1.0 Hz.

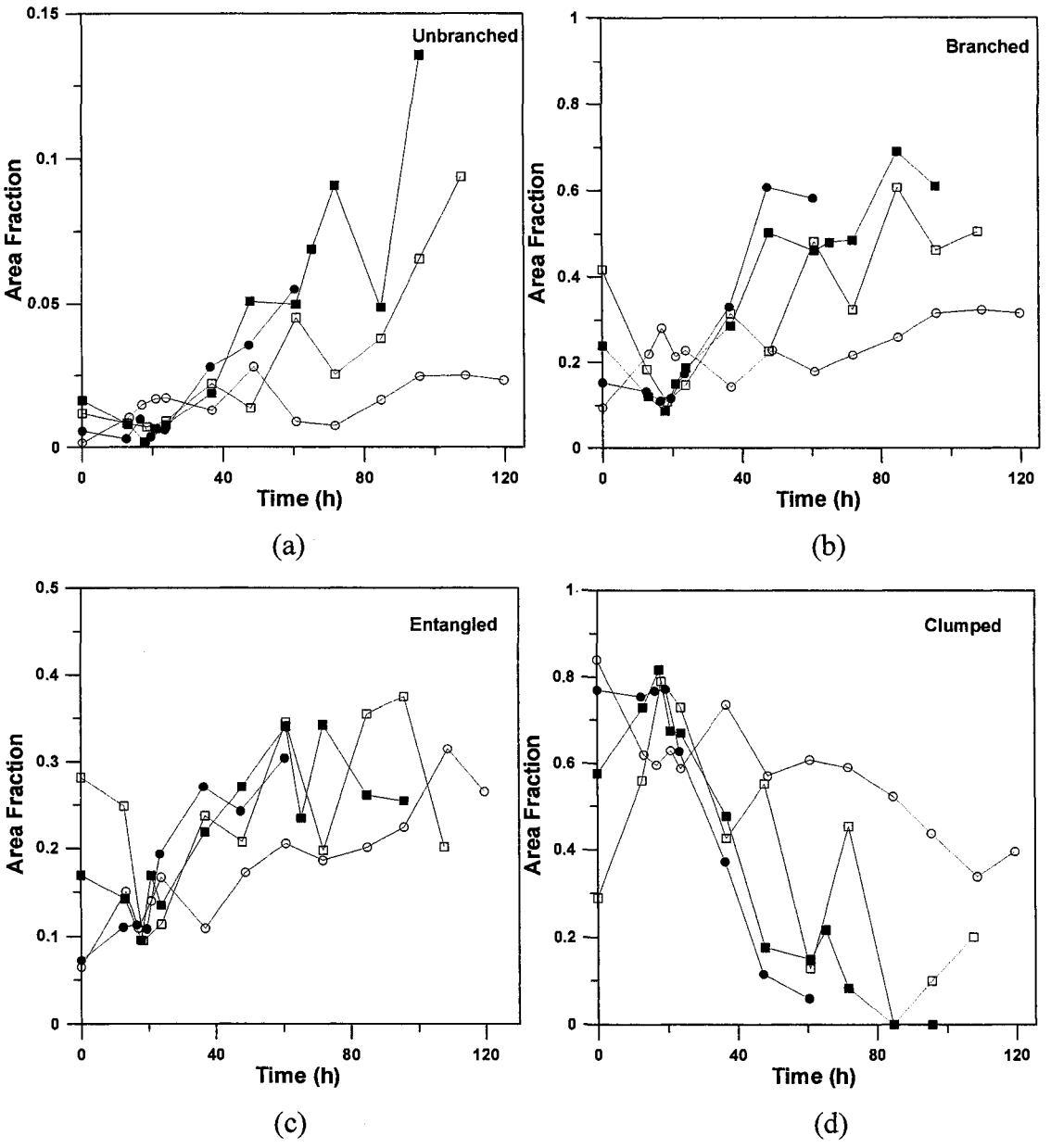

Figure E.3. Time profiles of area fractions of (a) unbranched (b) branched (c) entangled (d) clumped morphological states in STB at 300 RPM (●), 400 RPM (■), and in RPB at 0.50 Hz (o), and 0.75 Hz (□).

As explained in Chapter 2, the HGU tends to increase during the exponential growth phase and to decrease at the end of the batch phase. This trend is very obvious when the microorganism is grown in the STB (Figure E.4a). In the RPB (Figure E.4b), the same trend is observed for 0.50, 0.75 and 1.0 Hz. At 0.25 Hz, there is a sudden increase after 50 h because of growth. The biomass increased between 50 to 90 h.

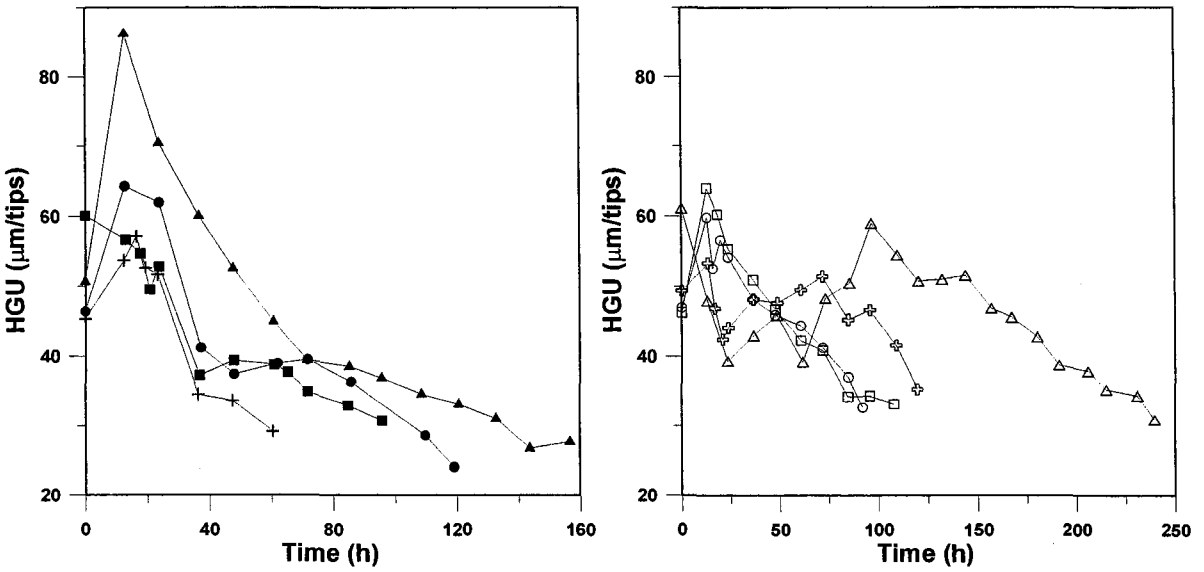

Figure E.4. Profiles of the average hyphal growth unit versus fermentation time in (a) STB at 200 (▲), 300 (+), 400 (●) and 500 (■) RPM; (b) RPB at 0.25 (Δ), 0.50 (+), 0.75 (o) and 1.0 (□) Hz.